We are IntechOpen,
the world's leading publisher of
Open Access books
Built by scientists, for scientists

6,900
Open access books available

186,000
International authors and editors

200M
Downloads

Our authors are among the

154
Countries delivered to

TOP 1%
most cited scientists

12.2%
Contributors from top 500 universities

CLARIVATE ANALYTICS

BOOK CITATION INDEX

INDEXED

WEB OF SCIENCE™

Selection of our books indexed in the Book Citation Index
in Web of Science™ Core Collection (BKCI)

Interested in publishing with us?
Contact book.department@intechopen.com

Numbers displayed above are based on latest data collected.
For more information visit www.intechopen.com

Li⁺ in Bipolar Disorder – Possible Mechanisms of Its Pharmacological Mode of Action

Carla P. Fonseca[1,2], Liliana P. Montezinho[1,3] and
M. Margarida C.A. Castro[1*]
[1]Dept. of Life Sciences, Faculty of Sciences and Technology, University of Coimbra;
Center for Neurosciences and Cell Biology (CNC) of Coimbra, Coimbra,
[2]CICS-UBI–Health Sciences Research Centre, University of Beira Interior, Covilhã,
[3]Dept. of Neurodegeneration 1, H. Lundbeck A/S, Valby,
[1,2]Portugal
[3]Denmark

1. Introduction

Bipolar disorder is a severe psychiatric illness characterized by cyclic episodes of mania and depression that affects approximately 1 % of the world population, and has a great economic and social impact. Lithium (Li⁺), in the form of lithium salts, has been used for more than five decades and is still the drug of choice in the treatment of this pathology. The anticonvulsants carbamazepine and valproate, originally used to treat epileptic seizures, are alternative or adjunctive therapies to lithium, representing the first-line therapy for lithium-resistant or lithium intolerant patients. Bipolar disorder is associated with structural, functional and physiological alterations in the brain of bipolar patients, which reflect chemical, neurochemical and metabolic changes, specifically at the levels of brain metabolites and neurotransmitters, as already detected by different techniques (Silverstone et al., 2005). Abnormalities in signal transduction pathways, in particular G proteins, adenylate cyclase (AC) and phosphatidylinositol (PI) signalling cascade, as well as protein kinase C (PKC) were related with the pathophysiology of bipolar disorder (Berns & Nemeroff, 2003, Brunello & Tascedda, 2003; Manji et al., 2001; Manji & Lenox, 2000a, 2000b).

Despite the widespread clinical use of lithium salts, the pharmacological mode of action underlying Li⁺ mood stabilizing effects is still unclear and several hypotheses have been advanced. Once inside the cells, Li⁺ has been proposed to compete with Na⁺ and Mg²⁺ for these ions intracellular binding sites in biomolecules, to affect intracellular Ca²⁺ concentration and to have an important role on the activity of G proteins, AC and inositol monophosphatase (IMPase) thus interfering with the levels of neurotransmitters and other substances in brain. Li⁺ has also been proposed to modulate the activity of certain glycolytic and tricarboxylic acid (TCA) cycle enzymes affecting several metabolic pathways and

---

*Corresponding author

altering the concentrations of intermediary metabolites. Recent research has been focused on how Li^+ changes the activity of cellular signal transduction systems, in particular those involving AC. The present chapter is a review of data published in literature from studies carried out to test some of these hypotheses, which, in most cases, are inter-related. The objective is to give an overview of what is known about possible mechanisms of Li^+ therapeutic action in bipolar disorder, at the molecular and cellular levels, using different approaches and techniques.

Li^+ effects have been shown to be highly cell-type specific and so the study of Li^+ transport processes across cell membranes is pertinent. Studies of the kinetics of Li^+ influx, intracellular immobilisation and Li^+/Mg^{2+} competition in different types of cells are presented (Amari et al., 1999a; Castro et al, 1996; Fonseca et al., 2000, 2004; Layden et al., 2003; Montezinho et al., 2002; Mota de Freitas et al., 2006; Nikolakopoulos et al., 1998). Li^+ influx rate constants were determined by atomic absorption spectrophotometry (experiments performed in cell suspensions) and ^7Li nuclear magnetic resonance (NMR) spectroscopy (cells immobilized in agarose), in the presence and absence of different activators and inhibitors of transport pathways present in these cells membrane. L-type voltage-sensitive Ca^{2+} channels were found to have an important role in Li^+ uptake under depolarising conditions in excitable cells. Once inside the cells, Li^+ was found to be bound to intracellular structures, as demonstrated by the ratio between the intracellular ^7Li NMR longitudinal and transversal relaxation times (T_1/T_2 ratio). The degree of intracellular Li^+ immobilisation is cell type dependent. Intracellular Mg^{2+} was found to be significantly displaced by Li^+ from its binding sites, as demonstrated by ^{31}P NMR and fluorescence spectroscopy (Fonseca et al., 2004)

The study of the effects of Li^+ on metabolic pathways is also referred. Results for Li^+ effects on glucose metabolism and on the competitive metabolism of glucose and lactate in a cell line, the human neuroblastoma SH-SY5Y cells, using ^{13}C NMR spectroscopy are presented (Fonseca et al., 2005). A relatively simple metabolic network was proposed for these cells, based on the computer program tcaCALC best fitting solutions. The results obtained suggested that cell energetic metabolism might be an important target for Li^+ action. ^{13}C NMR spectroscopy was also used to investigate Li^+ effects on glucose and acetate metabolism in primary cell cultures, rat cortical neurons and astrocytes, as well as in rat brain (Fonseca et al., 2009). It was proposed that Li^+ has an important role on the GABAergic neurotransmitter system as detected in cortical neurons when ^{13}C-glucose was used as substrate, as well as in rat brain after infusion with [1-^{13}C]glucose.

Since it has been suggested that cyclic adenosine 3',5'monophosphate (cAMP) levels are abnormal in bipolar patients and are regulated by mood stabilizing agents, it is of utmost importance to know whether this second messenger regulates Li^+ transport into neurons. It is also relevant to determine Li^+ effects on the homeostasis of intracellular cAMP levels. The effect of different intracellular cAMP levels on Li^+ uptake, at therapeutic plasma concentrations, was studied using pertinent cellular models and a radioactive assay (Montezinho et al., 2004). The data obtained demonstrated that intracellular cAMP levels regulate the uptake of Li^+ in a Ca^{2+} dependent manner, and that Li^+ plays an important role in the homeostasis of this second messenger in neuronal cells .

Second messenger-mediated pathways are targets for Li^+ action, thus, it is important to investigate whether other mood stabilizing agents exert similar effects on the same signalling pathways. Bipolar disorder seems to be associated with an enhanced signalling activity of the cAMP cascade and most of its events have been implicated in the action of mood stabilizing agents. Therefore the effects of Li^+, carbamazepine and valproate on basal and forskolin-evoked cAMP accumulation and the capacity of dopamine D_2-like receptors stimulation, with quinpirole, to block the increase of forskolin-stimulated cAMP levels were studied both *in vitro*, in cultured cortical neurons, and *in vivo* in the rat prefrontal cortex using microdialysis in freely moving animals, under control conditions and after treatment with the mood stabilizing drugs (Montezinho et al., 2006).

Several studies have suggested the involvement of biogenic monoaminergic neurotransmission in bipolar disorder and in the therapies used for this disease. The effects of the mood stabilizing drugs Li^+, carbamazepine or valproate on the dopaminergic and adrenergic systems, particularly on dopamine D_2-like and β-adrenergic receptors, were studied both in cultured rat cortical neurons and in the rat prefrontal cortex using microdialysis in freely moving animas (Montezinho et al., 2007). It was observed that these receptors have a regulatory role on AC activity and each drug acts by a unique mechanism. Dopamine D_2 and $β_1$-adrenergic receptors were found to be co-localized in cells of the prefrontal cortex, as determined by immunohistochemistry and were differentially affected by treatment with the three mood stabilizers, as determined by Western blot experiments. Data showed that the mood stabilizers studied affected dopamine D_2 receptors.

Figure 1 summarizes the possible targets for Li^+ action.

2. Characterisation of Li⁺ transport pathways and intracellular binding: Effects on Li⁺/Mg²⁺ competition in cellular models

Li^+ transport, intracellular immobilisation and Li^+/Mg^{2+} competition were studied in chromaffin cells, isolated from the bovine adrenal medulla, which are good neuronal models (Trifaró, 1982), and human neuroblastoma SH-SY5Y cells, a clonal derivative of the SK-N-SH cell line that provides a suitable model of neurons due to its exclusive neuroblast phenotype (Biedler et al, 1973). The results obtained and the main conclusions are presented in the following sections.

2.1 Li⁺ membrane transport studies in neuronal models

Atomic Absorption (AA) spectrophotometry was used to investigate the membrane transport pathways involved in the uptake of Li^+ by chromaffin cells (Fonseca et al., 2004). Figure 2 shows the kinetics of Li^+ influx in the control situation, in the presence of ouabain (a (Na^+, K^+)-ATPase inhibitor), and under continuous depolarising conditions in the absence and presence of nitrendipine (a specific blocker of the L-type voltage-sensitive Ca^{2+} channels). The kinetics of Li^+ influx was analysed using the following equation:

$$([Li^+]_{iT})_t = ([Li^+]_{iT})_\infty [1 - \exp(-k_i t)] \qquad (1)$$

where k_i is the rate constant for Li^+ influx, $([Li^+]_{iT})_t$ and $([Li^+]_{iT})_\infty$ are the total intracellular Li^+ concentrations at the different time points t and when the steady state has been reached, respectively.


(A)   (B)
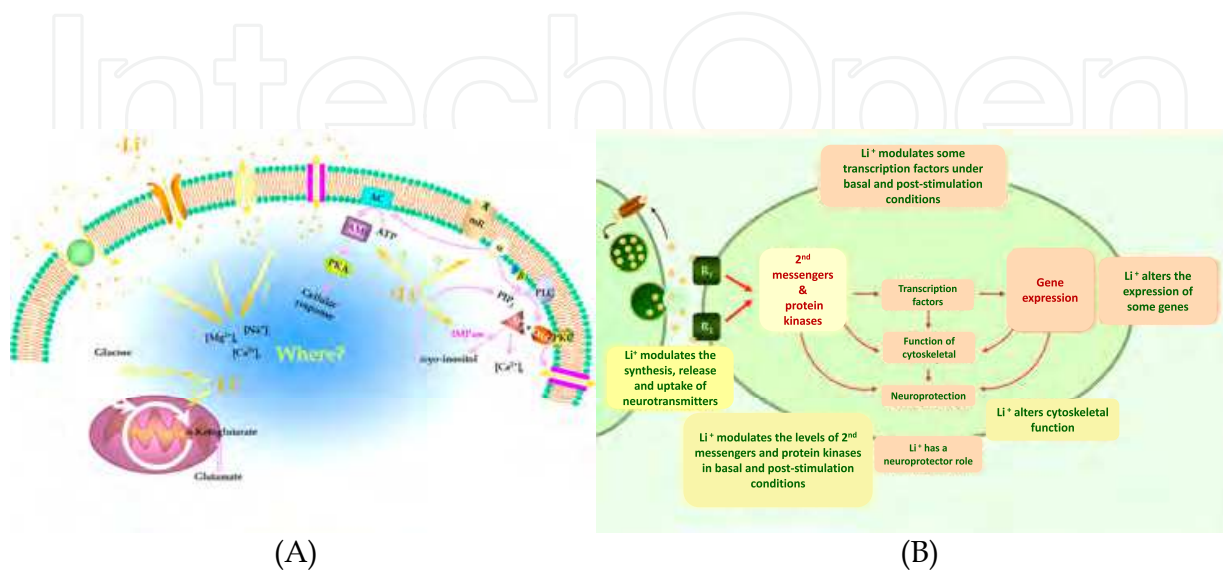
Fig. 1. Some potential targets for Li^+ action inside the cells. **A)** Li^+ is transported across the cell membrane, through specific transport systems already present in the membrane or by passive diffusion. Li^+ has been proposed to bind the negatively charged groups of several membrane phospholipids modulating the activity of membrane proteins and possibly ion transport processes. Li^+ can also affect the intracellular Ca^{2+} concentration $([Ca^{2+}]_i)$ and compete with mono- and di-cations, such as Na^+ and Mg^{2+}, respectively, for their intracellular binding sites. Other possible targets for Li^+ action are guanine-nucleotide binding proteins (G-proteins), adenylate cyclase (AC) and inositol monophosphatase (IMPase), affecting in this way the levels of second messenger molecules such as 3´,5´-cyclic adenosine monophosphate (cAMP), diacylglycerol (DAG) or inositol 1,4,5-triphosphate (IP_3), and the metabolism of phosphatidylinositols. Li^+ has also been proposed to modulate the activity of some glycolytic and tricarboxylic acid (TCA) cycle enzymes and the levels of some metabolic intermediates. α, β and γ – subunits of G-proteins; A – agonist; ATP – adenosine triphosphate; mR – metabotropic receptor; $[Mg^{2+}]_i$ and $[Na^+]_i$ – intracellular Mg^{2+} and Na^+ concentrations, respectively; PIP_2 – phosphatidylinositol 4,5-bisphosphate; PKA – protein kinase A; PKC – protein kinase C; PLC – phospholipase C. **B)** It is known that multiple inter-related neurotransmitter systems are involved in mood regulation. Thus, Li^+ can affect the functional equilibrium between several interacting systems. This figure shows the processes which seem to have an important role in the mechanisms of mood stabilization. R_1, R_2= post-synaptic receptors; ● = neurotransmitters (Jope, 1999a; Manji et al., 1995; Manji et al., 2001)

Experimental conditions	k_i (min^{-1})	$[Li^+]_{iT}$ (mmol (L cells)$^{-1}$)
Control	0.040 ± 0.006 (n=14)	11.39 ± 0.56
+ 50 μmol L^{-1} ouabain	0.036 ± 0.005 (n=7)	8.38 ± 0.38*
+ 45 mmol L^{-1} KCl	0.110 ± 0.038 (n=5)**	4.16 ± 0.27***
45 mmol L^{-1} KCl + 10 μmol L^{-1} nitrendipine	0.038 ± 0.007 (n=8)#	4.14 ± 0.28

(A)   (B)
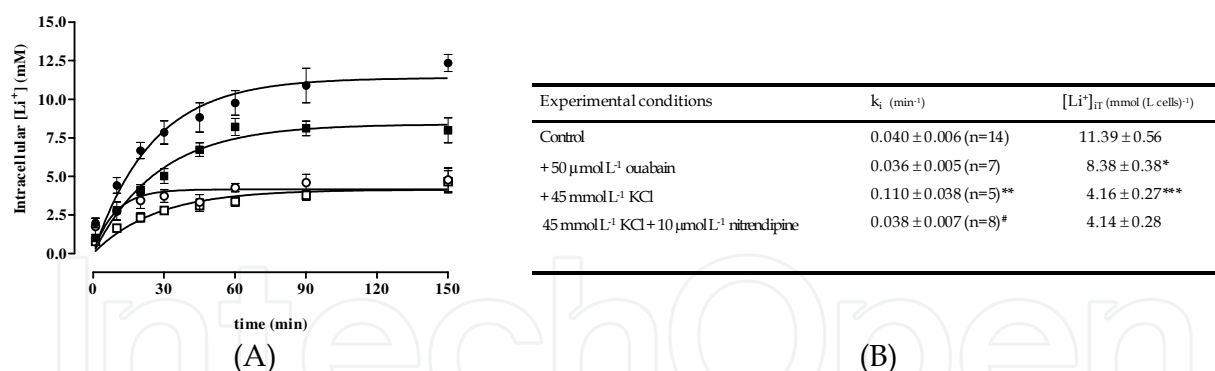
Fig. 2. **A)** Graphical representation of the $[Li^+]_{iT}$ (determined by AA spectrophotometry) *versus* loading time during Li$^+$ influx experiments in bovine chromaffin cells in suspension (cytocrit of 2 to 3%) subject to loading with 15 mmol L^{-1} Li$^+$, at 37 ºC. Data are for control (●), in the presence of 50 μmol L^{-1} ouabain (■), in the presence of 45 mmol L^{-1} KCl, a depolarising agent (○), and in the presence of 45 mmol L^{-1} KCl and 10 μmol L^{-1} nitrendipine (□). The lines correspond to the best exponential fits of the data to equation 1. In all cases, the intracellular Li$^+$ concentration increases up to 60–90 min and then reaches a steady state, except for the experiment done under depolarising conditions without nitrendipine, where the steady state is reached at 30 min; **B)** Li$^+$ influx rate constants (k_i) and the steady state total intracellular Li$^+$ concentrations ($[Li^+]_{iT}$), obtained from the curves presented in A), using equation 1. The values are average $\pm$ SEM for the number (n) of trials indicated in parenthesis. *, ** and ***: $p < 0.05$, $p < 0.01$ and $p < 0.001$ relative to control, respectively; # $p < 0.05$ relative to the KCl condition. (Fonseca et al., 2004)

In these experiments, the kinetics of Li$^+$ influx is not affected by the presence of ouabain, which suggests the non-involvement of (Na$^+$,K$^+$)-ATPase in Li$^+$ uptake by chromaffin cells, under resting conditions. However, when the cells are depolarised with KCl, a significant increase in the k_i value is observed, an effect that is completely suppressed in the presence of nitrendipine. This indicates that, under increased cellular excitability conditions, a new contribution to Li$^+$ influx appears which results from the activation of L-type voltage-sensitive Ca^{2+} channels. When the cells are depolarised, the intracellular Ca^{2+} concentration largely increases, increasing the activity of the Na$^+$/Ca^{2+} exchanger, known to be a high–capacity, low-affinity mechanism of Ca^{2+} efflux (Kao & Cheung, 1990; Powis et al., 1991). In our experiments, we propose that the Na$^+$/Ca^{2+} exchanger uses the external Na$^+$ and Li$^+$ to remove intracellular Ca^{2+} accumulated during cell depolarisation. Blocking of the L-type voltage-sensitive Ca^{2+} channels by nitrendipine prevents the depolarisation-dependent Ca^{2+} entry through these channels and therefore depresses the activity of the Na$^+$/Ca^{2+} exchanger, suppressing this new Li$^+$ entry pathway.

In the absence of active transport pathways for Li$^+$ influx, the $[Li^+]_{iT}$ obtained by AA spectrophotometry reflect the capacity of the cells to accumulate Li$^+$, which is controlled by the plasma membrane potential (-55mV in these cells, under resting conditions (Friedman et al.,1985)). When depolarisation occurs, the membrane potential becomes less negative, and the total amount of Li$^+$ that can be accumulated by the cells is lowered due to charge effects (Figure 2). This explains why the amount of Li$^+$ accumulated by the cells is significantly lowered when they are directly depolarised by KCl. The $[Li^+]_{iT}$ values observed under direct depolarising conditions in the presence and in the absence of nitrendipine are not significantly different, as expected, since under these conditions the membrane potential is

kept constant by the high extracellular K^+ concentrations, even if nitrendipine affects the Li^+ uptake kinetics. The observation that ouabain lowers the steady state $[Li^+]_{iT}$ also shows its depolarising effect on these cells (Kitayama et al.,1990).

2.2 Li^+ degree of immobilisation inside cells by ^7Li NMR

The degree of immobilisation of Li^+ within different types of cells was investigated using ^7Li NMR relaxation measurements when the intracellular Li^+ concentration has reached a steady-state. Therefore, Li^+ uptake was first followed by ^7Li NMR spectroscopy, along with the shift reagent $[Tm(HDOTP)]^{4-}$ in cell suspensions and in agarose-embedded and perfused cells. The shift reagent was used to separate ^7Li NMR signals corresponding to Li^+ inside and outside the cells (Nikolakopoulos et al., 1998; Rong et al., 1993). Figure 3 shows ^7Li NMR spectra from an influx experiment performed in agarose gel-embedded bovine chromaffin cells, under the experimental conditions indicated in figure legend. A graphical representation of the percent of intracellular ^7Li resonance area, A_i, relative to the total area of intra- and extracellular ^7Li resonances, $A_i + A_e$, over time is shown in Figure 3 C. The kinetics of Li^+ influx was defined by equation 2:

$$[(A_i)_t / (A_i + A_e)_t] = [(A_i)_\infty / (A_i + A_e)_\infty] [1 - \exp(-k_i t)] \qquad (2)$$

where k_i is the rate constant for Li^+ influx, $(A_i)_t$, $(A_e)_t$ and $(A_i)_\infty$, $(A_e)_\infty$ are the areas of the intracellular and extracellular $^7Li^+$ NMR signals at the different times t and when the intracellular Li^+ concentration has reached a steady state, respectively.
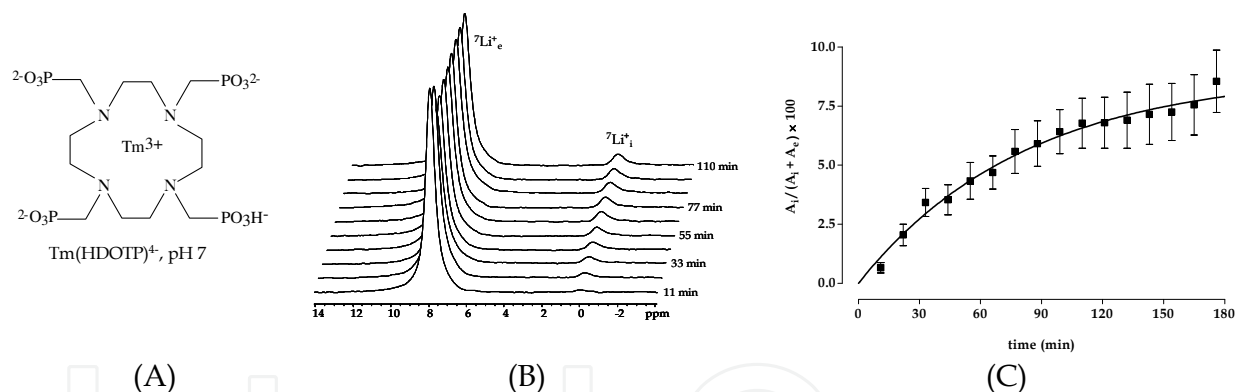

Fig. 3. **A)** Chemical structure of $[Tm(HDOTP)]^{4-}$; **B)** ^7Li NMR spectra (194.3 MHz) obtained over time in a Li^+ influx experiment performed with agarose gel-embedded bovine chromaffin cells (50 to 75 × 10⁶) continuously perfused, at 1 mL min⁻¹, with culture medium containing 15 mmol L⁻¹ Li^+ and 7 mmol L⁻¹ $[Tm(HDOTP)]^{4-}$ (37 °C). Each spectrum represents the average of the total accumulation time of 11 min. $^7Li^+_e$ and $^7Li^+_i$ are the extra- and intracellular ^7Li NMR resonances, respectively. NMR experiments were performed on a Varian Unity-500 NMR spectrometer equipped with a multinuclear 10 mm broadband probe and a controlled temperature unit, using the following parameters: 64 transients for each spectrum, spectral width of 5.6 kHz, pulse width of 15 μs, acquisition time of 0.360 s and recycling time of 10.36 s. The signal-to-noise ratio was enhanced by exponential multiplication with a line broadening of 30 Hz. **C)** Time dependence of the percentage of intracellular $^7Li^+$ NMR signal area, normalised to the total area of intra- and extracellular ^7Li NMR signals $[(A_i)/(A_i + A_e)]$. The experimental data was fitted using equation 2 and the line corresponds to the best exponential fit of the data (Fonseca et., 2004).

For chromaffin cells immobilised in agarose gel threads, the influx rate constant has a contribution from the diffusion process of Li^+ across the gel before reaching the cell membrane (Nikolakopoulos et al., 1996). Therefore, under these conditions, the value obtained from equation 2 for Li^+ influx is an apparent k_i value, k_{iapp}. The average value obtained for k_{iapp} was 0.012 ± 0.003 min^{-1}, much lower than the value determined for cell suspensions using AA spectrophotometry (0.040 ± 0.006 min^{-1}, Figure 2 B, (Fonseca et al., 2004)) or ^7Li NMR spectroscopy (0.040 ± 0.003 min^{-1}, (Fonseca et al., 2000)), as expected.

Three hours after the beginning of the $^7Li^+$ influx NMR experiments, when the steady state intracellular Li^+ concentration was reached, the degree of immobilisation of Li^+ inside different types of cells was investigated using ^7Li NMR relaxation measurements by determining intracellular $^7Li^+$ T_1 and T_2 values and the respective T_1/T_2 ratio. This ratio is a sensitive measure of the rotational correlation time, τ_c, of the Li^+ ion, and hence of Li^+ immobilisation, independently of the fraction of bound Li^+ and of its binding affinity (Layden et al., 2003; Nikolakopoulos et al., 1998; Rong et al., 1993) (Figure 4).
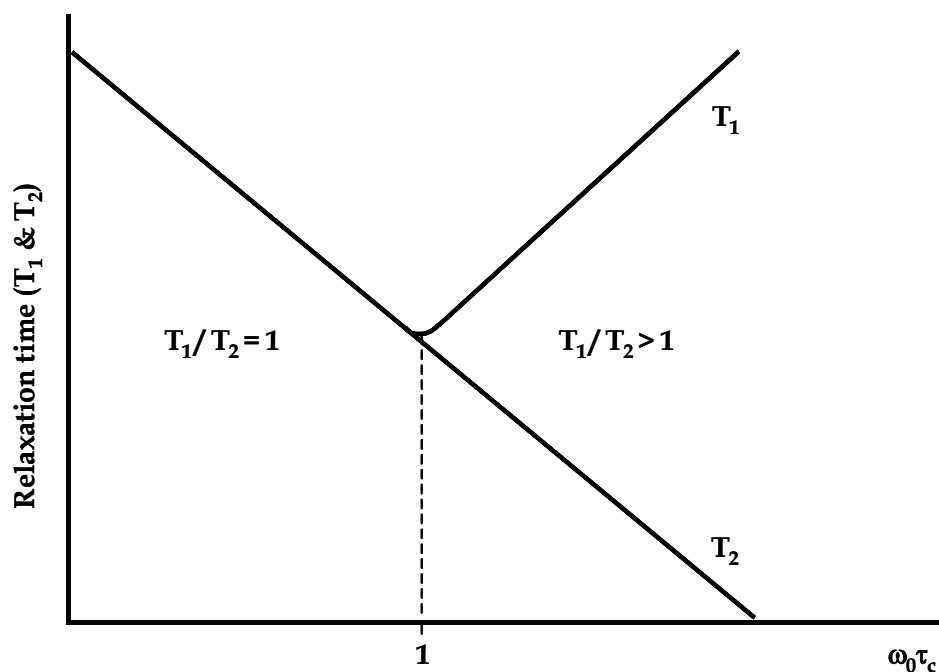

Fig. 4. T_1 and T_2 dependence on the rotational correlation time (τ_c) of a molecule. ω_0 stands for the Larmor angular frequency. When $\omega_0\tau_c \ll 1$ (for small molecules or freely moving ions) T_1 equals T_2 and the T_1/T_2 ratio equals 1. When $\omega_0\tau_c = 1$, T_1 reaches its minimum value and for $\omega_0\tau_c \gg 1$ (large molecules or immobilised ions) T_1 increases proportionally to τ_c while T_2 decreases and the T_1/T_2 ratio becomes higher than 1 (Adapted from Gil & Geraldes, 1987).

Table 1 compares the results obtained for different types of cells:

Sample	$[Li^+]$ [b]	T_1 (s)	T_2 (s)	T_1/T_2
Bovine chromaffin cells suspensions (n=5) [c]	1.7	6.1 ± 0.2	0.02 ± 0.002	305 ± 32
Bovine chromaffin cells perfused (n=4) [d]	11.4	5.4 ± 1.3	0.05 ± 0.006	106 ± 28
Neuroblastoma cells (n=3) [e]	2.9	5.1 ± 0.8	0.05 ± 0.02	102 [h]
Lymphoblastoma cells (n=3) [f]	3.1	2.6 ± 0.4	0.06 ± 0.01	43 ± 4
Human red blood cells (n=3) [g]	3.5	6.5 ± 0.2	0.46 ± 0.01	14 [h]
Viscosity adjusted LiCl solution [g,i]	4.0	3.9 ± 0.4	3.6 ± 0.6	1.1 ± 0.2

[a] Each T_1 and T_2 value is an average $\pm$ SEM for the number (n) of trials indicated in parenthesis. [b] For the cell samples, this is the steady state total intracellular Li^+ concentration of Li^+-loaded cells, $[Li^+]_{iT}$, expressed as mmol (L cells)$^{-1}$, with errors less than 10%. [c] Data from Fonseca et al., 2000. [d] Data from Fonseca et al., 2004. [e] Data from Nikolakopoulos at al., 1998. [f] Data from Layden at al., 2003. [g] Data from Rong et al., 1993. [h] Errors are less than 10%. [i] Sample viscosity was adjusted to 5 centipoise (cP) with glycerol.

Table 1. ^7Li NMR relaxation time[a] and T_1/T_2 ratio values for intracellular Li^+ obtained for different types of cells.

The T_1/T_2 ratio obtained for bovine chromaffin cells, under the perfusion experimental conditions, is considerably lower than for the same cells in suspension at similar extracellular Li^+ concentrations (15 mmol L^{-1}) , indicating an increased degree of immobilization of Li^+ in the latter case. This difference could reflect some loss of viability of the cells during the NMR experiments in cell suspensions without perfusion. The disruption of the cell membrane and the probable nonintegrity of the cytoplasm may contribute to a higher immobilization of this ion through binding to the cytoplasmatic membrane and intracellular structures. Comparing the T_1/T_2 ratios of the various perfused cell systems at similar Li^+ loading levels (Table 1), the degree of Li^+ immobilization follows the following order: chromaffin $\approx$ neuroblastoma > lymphoblastoma > red blood cells (RBCs), reflecting the relative local mobility of the intracellular Li^+ binding sites of the different systems.

2.3 Monitorisation of agarose-embedded cells viability using ^{31}P NMR spectroscopy

Cell viability of the perfused agarose-embedded cells was monitored by obtaining ^{31}P NMR spectra during the time course of the ^7Li NMR experiments. Figure 5 shows representative ^1H-decoupled ^{31}P NMR spectra obtained after Li^+ NMR experiments in bovine chromaffin cells and neuroblastoma SH-SY5Y cells.

The criteria used to evaluate cell viability during the NMR experiments were, in the case of SH-SY5Y cells, the intracellular levels of ATP and PCr over the course of the perfusion experiments (by monitoring the areas of the PCr and of the α-, β-, and γ-ATP ^{31}P NMR resonances and the ratio of the PCr/β-ATP areas) and the chemical shift of inorganic phosphate (P_i) which is related to the intracellular pH of the sample. The areas of the ^{31}P NMR resonances of PCr and of ATP, as well as the chemical shift of the P_i resonance did not change appreciably during the course of NMR experiments, showing that there were no significant changes in energy metabolism or intracellular pH (Nikolakopoulos et al., 1998).
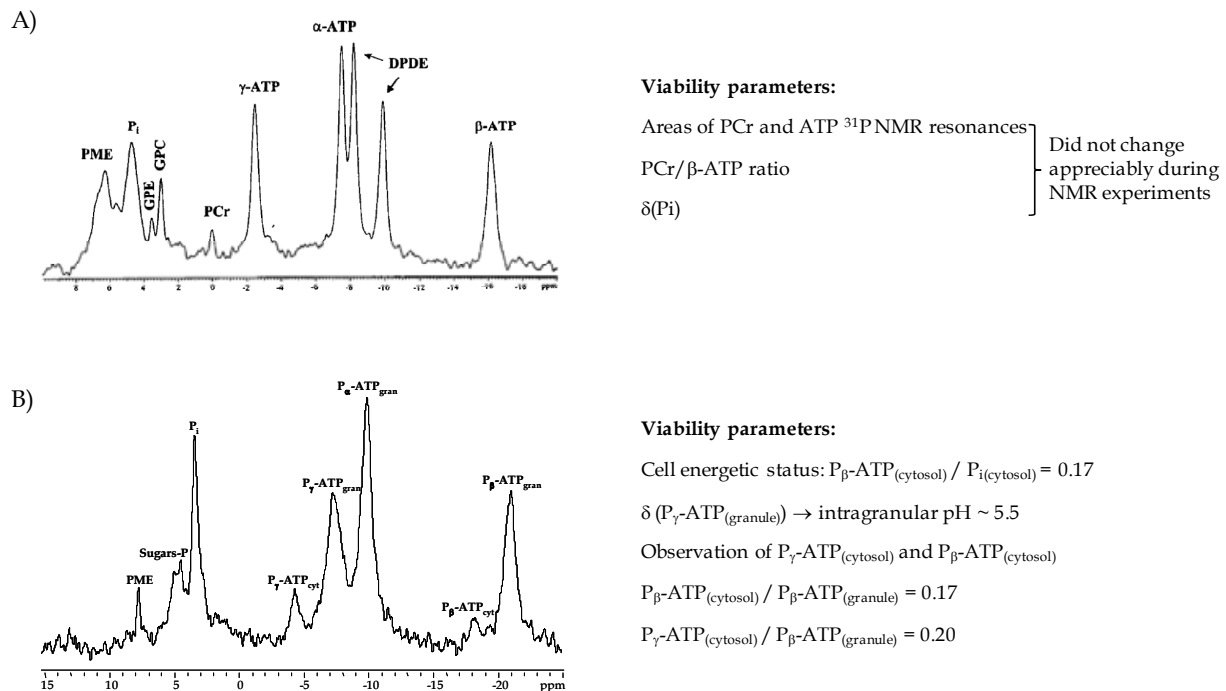
Fig. 5. ^{1}H-decoupled ^{31}P NMR spectrum (202.3 MHz) of Li⁺-loaded agarose gel-embedded SH-SY5Y cells, after 5 h perfusion (Nikolakopoulos et al., 1998) (**A**) or bovine chromaffin cells, after 7 h 30 min perfusion (Fonseca et al., 2004) (**B**). For SH-SY5Y cells, ^{31}P chemical shifts are reported relative to phosphocreatine (PCr) referenced at 0 ppm. For chromaffin cells, H_3PO_4 85% was used as an external reference (0 ppm). PME: phosphomonoesters; P_i: inorganic phosphate; GPE: glycerophosphorylethanolamine; GPC: glycerophosphorylcholine; PCr: phosphocreatine; DPDE: diphosphodiesters; Sugars-P: sugars phosphate groups; α- β- and γ-ATP: α, β and γ phosphate groups of ATP; $P_β$– and $P_γ$–ATP_{cyt}: β and γ phosphate groups, respectively, of cytosolic ATP; $P_α$–, $P_β$– and $P_γ$–ATP_{gran}: α, β and γ phosphate groups of granular ATP, respectively.

In contrast to the SH-SY5Y cells, the ^{31}P NMR spectrum of perfused bovine chromaffin cells shows compartmentation of ATP in the cytosol and inside the granules. The ^{31}P NMR signal of cytosolic $P_α$-ATP is not observable, as it is part of the composite peak at – 10.8 ppm with the resonance from intragranular $P_α$-ATP, as well as from the vesicular $P_α$-ADP and the bisphosphate moiety of NAD⁺ and NADH (Painter et al., 1989). In the particular case of chromaffin cells, the criteria used to evaluate cell viability were the ratio of the areas of the $P_β$-$ATP_{(cytosol)}$ and $P_{i(cytosol)}$ ^{31}P NMR resonances ($P_β$-$ATP_{(cytosol)}$/$P_{i(cytosol)}$) (which reflects the energetic state of the cells (Kaplan et al., 1989)), the chemical shift of the $P_γ$-$ATP_{(granule)}$ resonance (which is related to the intragranular pH (Njus et al., 1978)), the observation of the cytosolic $P_γ$-ATP and $P_β$-ATP signals (under good perfusion conditions, these resonances appear at approximately –4.5 and –18.4 ppm, respectively) and the area ratio $P_β$-$ATP_{(cytosol)}$/ $P_β$-$ATP_{(granule)}$. The analysis of these parameters, as shown in Figure 5B), showed that the energetic state and the viability of perfused chromaffin cells were kept throughout the NMR experiments (Fonseca et al., 2004).

2.4 Li$^+$/Mg^{2+} competition studies by ^{31}P NMR and fluorescence spectroscopy

It has been suggested that Li$^+$ may compete with Mg^{2+} (a very well-known protein cofactor) for Mg^{2+} binding sites in several biomolecules, due to their similar chemical properties. Li$^+$/Mg^{2+} competition have been studied in Mg^{2+}-dependent biomolecules (*e.g.* ATP, ADP, GTP, GDP, IP$_3$, G-proteins and phosphate groups of RBCs membrane phospholipids) and in cellular systems (such as Li$^+$-loaded human RBCs and lymphoblastoma cells) using fluorescence spectroscopy with the Mg^{2+} indicator furaptra, as well as ^{7}Li and ^{31}P NMR spectroscopy (Amari et al., 1999b; Layden et al., 1999, 2003; Mota de Freitas et al., 1994, 2006; Ramasamy et al., 1989; Rong et al., 1994; Srinivasan et al., 1999).

^{31}P NMR spectroscopic method was used to examine the competition between Li$^+$ and Mg^{2+} ions within intact human neuroblastoma SH-SY5Y cells. The ^{31}P NMR method is based on the measurement of chemical shift difference changes between the ^{31}P NMR resonances of the P$_\beta$ and P$_\alpha$ phosphate groups ($\Delta\delta_{\alpha\beta}$) of ATP due to Mg^{2+} binding (Gupta et al., 1978). Upon Mg^{2+} binding to ATP, the β phosphate resonance is shifted downfield and the chemical shift difference between the β and α phosphates decreases (Amari et al., 1999a), being a parameter indicative of Mg^{2+} binding to ATP and used to measure Li$^+$/Mg^{2+} competition. The values of $\Delta\delta_{\alpha\beta}$ were taken from ^{31}P NMR spectra of Li$^+$-loaded (Figure 5A) and Li$^+$-free SH-SY5Y cells, and used to calculate intracellular free Mg^{2+} concentrations, [Mg^{2+}]$_f$, in both situations, as described in (Amari at al.,1999a). We found that the αβ chemical shift in Li$^+$-free cells was 8.67 ± 0.02 ppm (n=3), whereas in Li$^+$-loaded cells this difference increased significantly (p<0.0005) to 8.87 ± 0.02 ppm (n=3), corresponding to a [Mg^{2+}]$_f$ of 0.35 ± 0.03 mmol L^{-1} and 0.80 ± 0.04 mmol L^{-1}, respectively (Amari et al.,1999a). The increase in [Mg^{2+}]$_f$ after Li$^+$ loading suggests that Li$^+$ may compete with Mg^{2+} for its binding sites within the neuroblastoma cells.

The ^{31}P NMR method could not be used to study Li$^+$/Mg^{2+} competition in bovine chromaffin cells due to some particular characteristics of these cells. In fact, ATP compartmentation in chromaffin cells causes the overlap of the P$_\alpha$ ^{31}P NMR signals of cytosolic and granular ATP (Figure 5), preventing the use of this technique to determine [Mg^{2+}]$_f$ in the cytosol of these cells. Concerning the granule, no effect of Li$^+$ loading on the granular $\Delta\delta_{\alpha\beta}$ value was observed, indicating no significant Li$^+$/Mg^{2+} competition inside this organelle. Therefore, fluorescence spectroscopy using the Mg^{2+}-specific fluorescent probe furaptra was the method of choice to study Li$^+$/Mg^{2+} competition in these cells. According to established data (Amari et al., 1999a, 1999b), an increase in the ratio of fluorescence intensities at 335 nm and 370 nm, R = (F$_{335}$/F$_{370}$), during Li$^+$ cell loading is indicative of the displacement of Mg^{2+} by Li$^+$ from its binding sites, increasing the amount of intracellular free Mg^{2+} available to bind to furaptra (salt form) inside the cells. The R values can be converted into [Mg^{2+}]$_f$ using equation 3, which corrects for Li$^+$ binding to furaptra:

$$[Mg^{2+}]_f = (K_d \, S_{min} \, (R - R_{min}) \, / \, S_{max} \, (R_{max} - R)) + \\ (K_d \, S'_{max} \, (R - R'_{max})[Li^+]_{if} \, / \, K'_d \, S_{max} \, (R_{max} - R)) \tag{3}$$

where R$_{min}$, R$_{max}$ and R$'_{max}$ are the ratios of the fluorescence intensities at 335 and 370 nm in the absence of metal ions and in the presence of saturating amounts of Mg^{2+} or Li$^+$, respectively; S$_{min}$, S$_{max}$ and S$'_{max}$ are the fluorescence intensities at 370 nm, respectively, in the absence of metal ions and in the presence of saturating amounts of Mg^{2+} or Li$^+$; K$_d$ and K$'_d$ are the dissociation constants of the furaptra-Mg^{2+} (1.5 mmol L^{-1} (Raju et al.,1989)) and

furaptra-Li+ (237 mmol L-1 (Amari et al., 1999b)) complexes, respectively. $[Li^+]_{if}$ is the intracellular free Li+ concentration, corresponding to the Li+ ions capable of competing with Mg^{2+} for furaptra (Amari et al., 1999b).

Figure 6 shows the fluorescence excitation spectra of furaptra in the presence of increasing concentrations of Mg^{2+} and a graphical representation of the time dependence of the R values for a control situation (in the absence of Li+) and for a 90 min Li+-loading experiment using a total Li+ concentration in the medium of 15 mmol L-1.
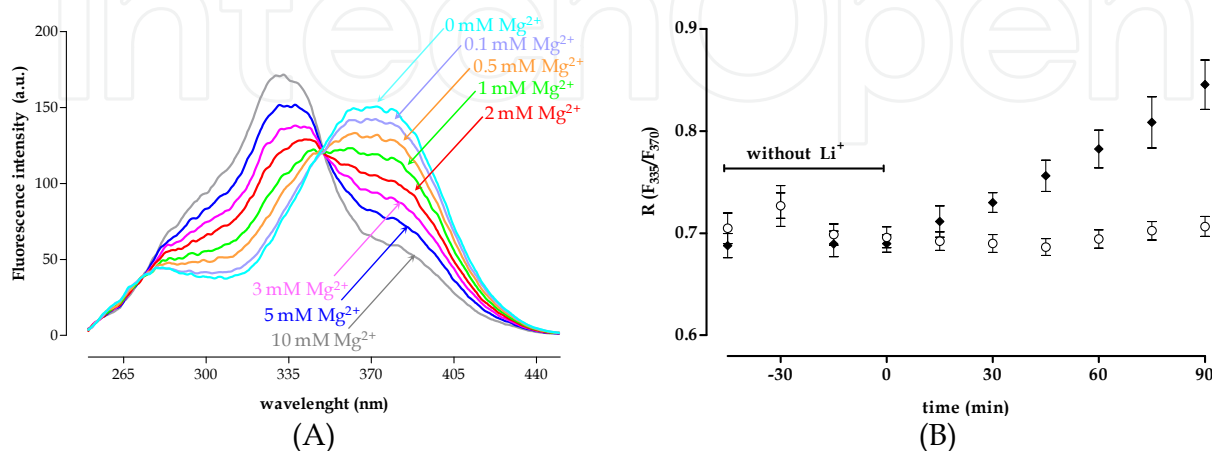
Fig. 6. **A)** Fluorescence excitation spectra of furaptra (0.2 μmol L-1) in a modified Krebs medium (in mmol L-1: NaCl 140, KCl 5, glucose 10, HEPES 20, EGTA 0.5, pH 7.35) containing 0-10 mmol L-1 free Mg^{2+}. The emission wavelength was fixed to 500 nm. The binding of Mg^{2+} to furaptra results in a blue shift in the excitation spectrum of this indicator from 370 to 335 nm with increasing amounts of Mg^{2+}. **B)** Time dependence of fluorescence intensity ratio R = (F_{335}/F_{370}) in bovine chromaffin cells previously loaded with furaptra, under control (Li+-free) conditions (○) and when the cells were incubated for 90 min with 15 mmol L-1 Li+ (◆). Bovine chromaffin cells, adherent to a 1 cm2 square poly-L-lysine coated coverslip (0.8 × 106 cells per cm2) were placed in a fluorescence cuvette containing Krebs medium (in mmol L-1: NaCl 140, KCl 5, $CaCl_2$ 2, $MgCl_2$ 1, glucose 10, HEPES 20, pH 7.35). In the Li+ experiment, this medium was then replaced by a modified Krebs medium containing 15 mmol L-1 Li+ (NaCl was partially replaced in order to maintain the osmolarity of the medium). During the experiments, the medium was changed every 15 min to remove any fluorescent probe that might have been released from the cells to the incubation medium, preventing the binding of the probe to the extracellular Mg^{2+}, which would contribute to an overestimated value of $[Mg^{2+}]_f$ (Fonseca et al., 2004).

In the absence of Li+, the basal R value, which corresponds to $[Mg^{2+}]_f$ = 0.54 ± 0.01 mmol (L cells)-1 (n = 12), was maintained over time for 135 min. In the presence of Li+, the $[Mg^{2+}]_f$ value was not significantly different from the control one ($[Mg^{2+}]_f$ = 0.52 ± 0.02 mmol (L cells)-1, n=6) at time zero of Li+ loading, but it significantly increased by 52% during the 90 min of the Li+ loading process to a value of 0.79 ± 0.05 mmol (L cells)-1 ($\Delta[Mg^{2+}]_f$ = 0.27 ± 0.05 mmol (L cells)-1). In $[Mg^{2+}]_f$ calculations it was considered the $[Li^+]_{if}$ = 9.42 ± 0.01 mmol (L cells)-1 obtained by 7Li NMR for immobilised, perfused cells at steady state, which was shown to be the most accurate value (Fonseca et al., 2004). The $[Mg^{2+}]_f$ increase when Li+ enters the viable cells, observed by fluorescence spectroscopy, confirms the capacity of Li+ to displace Mg^{2+} from its intracellular binding sites.

The relative extent of Li^+/Mg^{2+} competition, which is cell type and $[Li^+]_{iT}$ dependent, may expressed by the percent $[Mg^{2+}]_f$ increase divided by $[Li^+]_{iT}$ ($\%(\Delta[Mg^{2+}]_f/[Mg^{2+}]_f)/[Li^+]_{iT}$ ratio). This extent is higher for neuroblastoma cells, similar for chromaffin and lymphoblastoma cells, and lower for RBCs (Fonseca et al., 2004). Based on the relative percent $[Mg^{2+}]_f$ increase/$[Li^+]_{iT}$ ratio values reported above, we suggest that the extent of Li^+/Mg^{2+} competition under pharmacological conditions is cell-type dependent, being affected by differences in Li^+ transport and immobilisation properties.

Li^+/Mg^{2+} competition has been shown to occur at therapeutic intracellular Li^+ levels (0.6–3.1 mmol (L cells)$^{-1}$) in human neuroblastoma SH-SY5Y cells (Layden et al., 2000). Changes in $[Mg^{2+}]_f$ of the order of 10%, observed for these cells at $[Li^+]_i$ = 0.6 mmol (L cells)$^{-1}$, are expected to have a large impact on the many biochemical and cell signalling pathways involving Mg^{2+}-dependent enzymes (Layden et al., 2003). Based on the experimentally observed proportional relationships in $\%(\Delta[Mg^{2+}]_f/[Mg^{2+}]_f)/[Li^+]_i$, much smaller percentage (3%) effects in $[Mg^{2+}]_f$ are to be expected in chromaffin cells at $[Li^+]_i$ = 0.6 mmol (L cells)$^{-1}$, similar to those proposed for lymphoblastoma cells (3%) but still higher than for RBCs (1.5%) (Layden et al., 2003), which possibly will have an undetectable cell impact.

In summary, ^7Li NMR spectroscopy proved to be a useful tool to investigate Li^+ transport, along with AA spectrophotometry, and intracellular binding in cellular models, whereas ^{31}P NMR and fluorescence spectroscopy, using the Mg^{2+}-specific fluorescent probe furaptra, allowed to quantify intracellular competition between Li^+ and Mg^{2+} ions. These studies provide further evidence for the generality of the ionic competition mechanism, contributing to the understanding of the pharmacological action of Li^+ at the molecular level.

3. Metabolic effects of Li^+ on neuronal and glial cells and rat brain

3.1 Li^+ effects on cell energetic metabolism

Altered intracellular signalling systems are thought to play an important role in the pathophysiology of bipolar disorder (Jope, 1999b; Lenox & Hahn, 2000; Manji et al., 1995). Since these processes, as well as brain activity in general, closely depend on energy metabolism and ATP availability, changes in brain energy metabolism may also be involved in the pathogenesis of this disease. Neuroimaging techniques (mainly positron emission tomography and blood oxygen level-dependent (BOLD)-based functional magnetic resonance imaging (fMRI)) suggest that both mania and depression are associated with alterations in the rates of substrate oxidation by the brain (Caligiuri et al., 2003; Goodwin et al., 1997; Kennedy et al., 1997). Other methods such as ^{31}P magnetic resonance spectroscopy (MRS) have provided evidence for dysfunction at the level of brain cells intermediary metabolism (Deicken et al., 1995; Kato et al., 1993, 1998; Kato & Kato, 2000). Since cerebral oxygen consumption and ATP synthesis are both tightly coupled to TCA cycle activity, such changes likely represent significant changes in cellular TCA cycle flux.

The therapeutic effects of Li^+ may be related to modifications of cerebral intermediary metabolic rates. Therefore, we studied the effect of Li^+ on TCA cycle flux from exogenous glucose in human neuroblastoma SH-SY5Y cells, a neuronal model (Biedler et al, 1973). Also, in light of studies suggesting that lactate may be an important neuronal oxidative substrate (Bouzier-Sore et al., 2003; Pellerin & Magistretti, 2004), the effect of Li^+ on competition between exogenous lactate and glucose for TCA cycle oxidation in these cells

was also investigated. Modifications in the contribution of glucose and lactate to pyruvate and acetyl-CoA production could significantly alter the energy status of neuronal cells. Finally, the effect of Li^+ on the metabolism of glucose in primary cultures of cortical neurons and glial cells was also addressed.

3.1.1 Effects of Li⁺ on the intermediary metabolism of SH-SY5Y cells

The effects of Li^+ on glucose and lactate metabolism in human neuroblastoma SH-SY5Y cells were evaluated by ¹³C NMR isotopomer analysis, a powerful technique to study metabolic intermediary metabolism. Briefly, ¹³C-labelled substrates ([U-¹³C]glucose alone or a mixture of [U-¹³C]glucose and [3-¹³C]lactate) were used and allowed to be metabolised by the cells. Their fate was then deduced by ¹³C NMR analysis of metabolite isotopomer distributions. Relative pathways feeding the TCA cycle were estimated from the relative areas of glutamate C2, C3 and C4 multiplets in the ¹³C NMR spectra using the computer program tcaCALC (Malloy et al., 1988; Sherry et al., 2004). Figure 7 shows representative ¹H-decoupled ¹³C NMR spectra of SH-SY5Y cell extracts obtained under control conditions (absence of Li^+) after incubation for 24 h with [U-¹³C]glucose (Figure 7A) or a mixture of [U-¹³C]glucose plus [3-¹³C]lactate (Figure 7B).
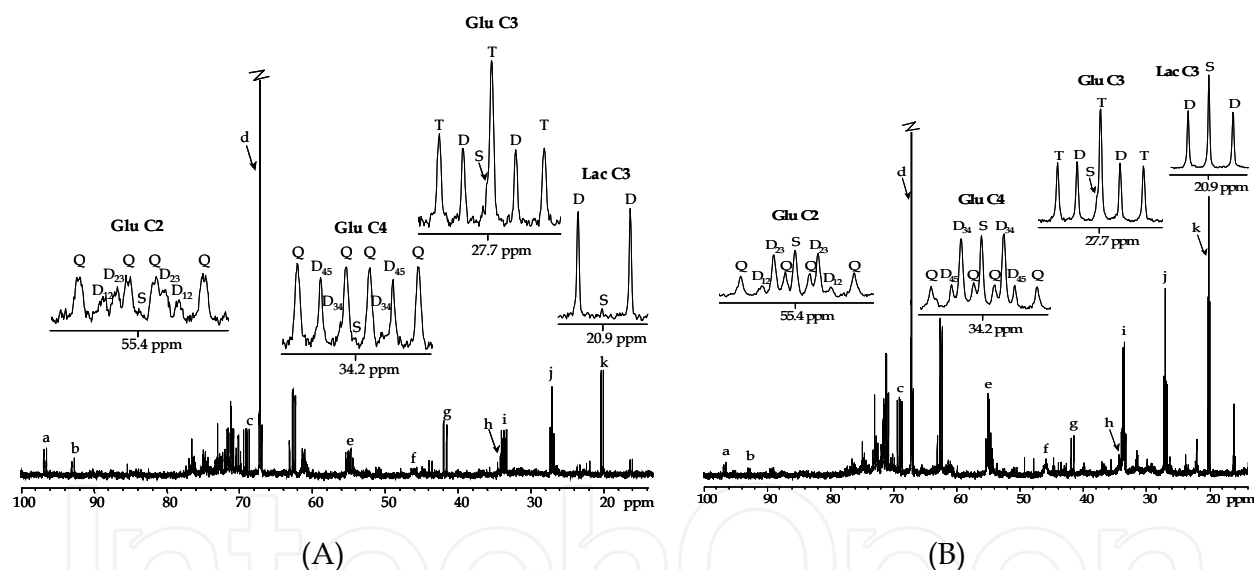
Fig. 7. Representative ¹H-decoupled ¹³C NMR spectra (125.7 MHz) from SH-SY5Y cell extracts obtained after incubating the cells for 24 h in Krebs-Ringer Bicarbonate (KRB) medium (in mmol L⁻¹: NaCl 119, KCl 4.7, $MgSO_4$ 1.2, KH_2PO_4 1.2, $CaCl_2$ 1.3, $NaHCO_3$ 24, pH 7.3) supplemented with 5 mmol L⁻¹ [U-¹³C]glucose (**A**) or a mixture of 5 mmol L⁻¹ [U-¹³C]glucose and 5 mmol L⁻¹ [3-¹³C]lactate (**B**), in the absence of Li^+ (control) (Fonseca et al., 2005). Carbon 2, 3 and 4 resonances of glutamate (Glu) and carbon 3 resonance of lactate (Lac) are expanded and assigned as follows: Q - quartet; T - triplet; D - doublet; D_{12} - doublet due to the coupling constant between carbons 1 and 2 (J_{12}) ~ 52 Hz; D_{23} - doublet due to J_{23} ~ 34 Hz; D_{34} - doublet due to J_{34} ~ 34 Hz; D_{45} - doublet due to J_{45} ~ 52 Hz; S - singlet. Resonance assignments: a – glucose C1 β; b – glucose C1 α; c – lactate C2; d – dioxane (reference, 67.4 ppm); e – glutamate C2; f – citrate C2,C4; g – malate C3; h – succinate C2,C2'; i – glutamate C4; j – glutamate C3; k – lactate C3.

[13]C-incorporation was mainly observed on glutamate and lactate resonances. As for many other tissues, glutamate was the most abundant ^{13}C-enriched metabolite at the level of TCA cycle intermediates. The complex [13]C-^{13}C splitting patterns, expanded in Figure 7 for C4, C3 and C2 glutamate resonances, reveal the presence of different groups of this metabolite isotopomers as a result of glutamate labelling in different positions. The areas of the glutamate C2, C3 and C4 resonances in the spectra were calculated and the results introduced in tcaCALC program in order to obtain the following relative metabolic parameters: lac_{123} (the fraction of acetyl-CoA derived from the oxidation of [U-^{13}C]pyruvate), lac_3 (fraction of acetyl-CoA derived from the oxidation of [3-^{13}C]pyruvate, *via* pyruvate dehydrogenase (PDH), when applicable), fat_0 (the fraction of acetyl-CoA derived from unlabelled acyl sources) and y (anaplerotic flux from all sources). Further details about this method can be found in Fonseca et al., 2005. For the neuroblastoma SH-SY5Y cells, the metabolic model shown in Figure 8 was the one that provided the best fit between the glutamate isotopomer information and metabolic flux parameters as defined by the Monte Carlo and other statistical analyses of tcaCALC.
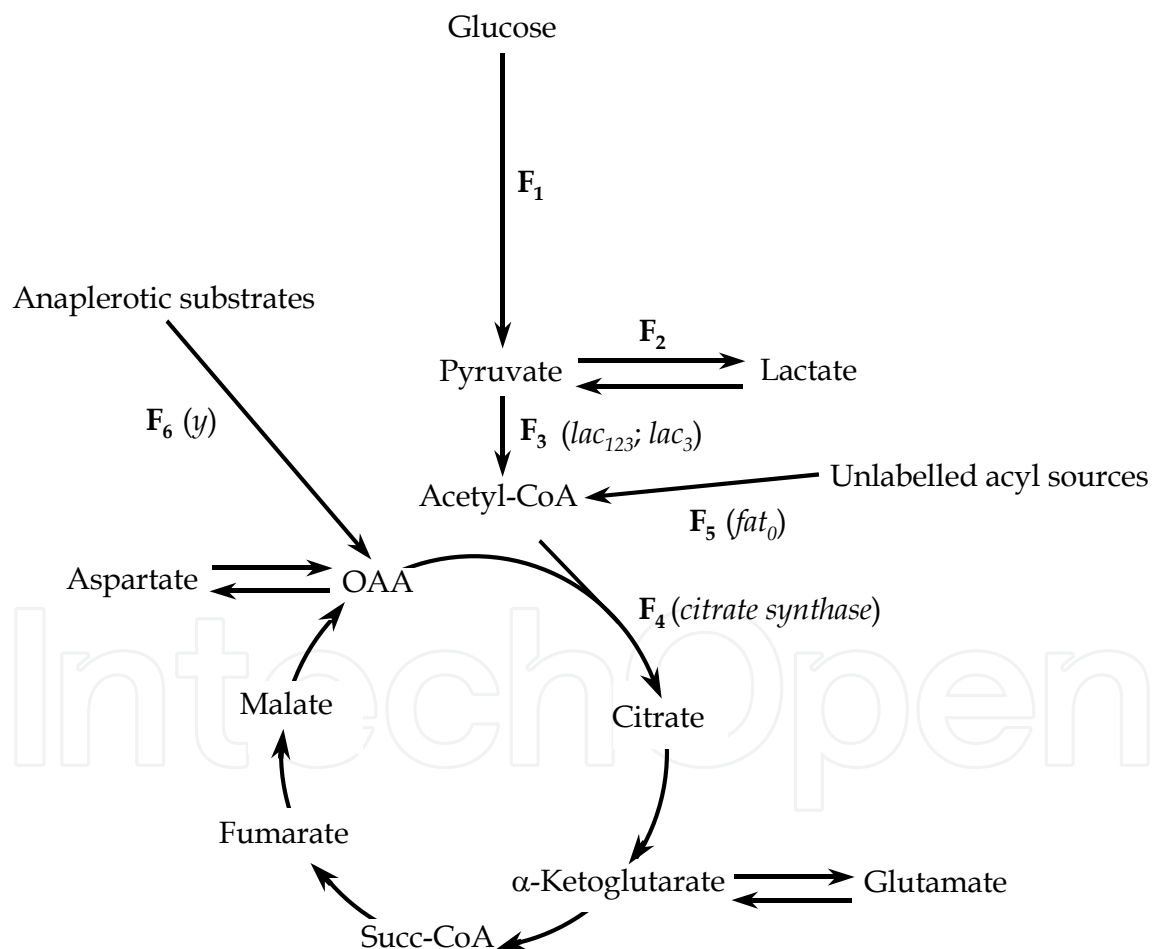
Fig. 8. Metabolic model for glucose and lactate metabolism in SH-SY5Y cells, based on tcaCALC best fitting solutions (Fonseca et al., 2005). The best fit was achieved with the parameter set of *lac123*, *y* and *fat0*. Note that *y* represents total flux from all anaplerotic pathways. Inclusion of carboxylation of labelled pyruvate and/or pyruvate cycling fluxes to the model did not significantly improve the fit; hence, these parameters were excluded .

Absolute TCA cycle fluxes were calculated using the following equations:

$$\text{Absolute PDH flux } (F_3) = \text{Total glucose utilisation } (F_1) - \text{Net lactate production } (F_2) \quad (4)$$

$$\text{Absolute citrate synthase flux } (F_4) = F_3 / lac_{123} \quad (5)$$

$$\text{Absolute endogenous acyl oxidation flux } (F_5) = fat_0 \times F_4 \quad (6)$$

$$\text{Absolute endogenous anaplerotic flux } (F_6) = y \times F_4 \quad (7)$$

Extracellular glucose and lactate concentrations along the experimental period and, hence, glucose consumption (F_1) and lactate production (F_2) rates were calculated using an enzymatic method coupled to the increase in NADH absorption at 340 nm. Table 2 summarises the absolute metabolic fluxes for SH-SY5Y cells incubated in the presence of 5 mmol L-1 [U-13C]glucose and the effects of 1 and 15 mmol L-1 Li+ on these fluxes.

Absolute metabolic fluxes (μmol h-1 mg-1 protein)	Control	1 mmol L-1 Li+	15 mmol L-1 Li+
Glucose consumption (F_1)	0.877 ± 0.362 (n=6)	0.540 ± 0.170 (n=6)	0.411 ± 0.107 * (n=5)
Lactate production (F_2)	0.268 ± 0.086 (n=6)	0.275 ± 0.047 (n=6)	0.267 ± 0.064 (n=6)
Pyruvate dehydrogenase (F_3)	0.609 ± 0.302 (n=6)	0.216 ± 0.076 * (n=5)	0.098 ± 0.043 ** (n=4)
Citrate synthase (F_4)	0.666 ± 0.331 (n=3)	0.246 ± 0.087 ** (n=3)	0.108 ± 0.047 ** (n=3)
Endogenous acyl oxidation (F_5)	0.057 ± 0.029 (n=3)	0.030 ± 0.011 * (n=3)	0.009 ± 0.004 ** (n=3)
Endogenous anaplerosis (F_6)	0.091 ± 0.047 (n=3)	0.025 ± 0.012 ** (n=3)	0.011 ± 0.006 ** (n=3)

Table 2. Absolute fluxes in SH-SY5Y cells incubated for 24 h at 37 °C in KRB medium containing 5 mmol L-1 [U-13C]glucose, in the absence (control) and presence of 1 or 15 mmol L-1 Li+ (Fonseca et al., 2005). Values are means ± SD for the number (n) of experiments indicated in parenthesis. Glucose consumption rates were multiplied by 2 to express consumption in triose units. * and **: p < 0.05 and p < 0.01 relative to control, respectively.

SH-SY5Y cells have a relatively simple metabolic network featuring a single pyruvate pool and no cycling between pyruvate and oxaloacetate (Figure 8). The presence of 1 or 15 mmol L-1 Li+ did not alter this optimal set of flux parameters. Under control conditions, TCA cycle oxidation accounted for about two-thirds of glucose consumption while the remaining third was converted to lactate. With Li+, glucose conversion into pyruvate decreased, which is consistent with an inhibition of glycolytic flux, as already reported in literature (Kajda et al., 1979; Kajda & Birch, 1981; Nordenberg et al., 1982; Zager & Ames III, 1988). This study indicates that despite the decrease in glucose consumption by Li+, lactate production rates were constant, which is consistent with an unchanged intracellular redox state. However, the fraction of glucose consumed by TCA cycle oxidation (given by the absolute PDH flux, F_3) was significantly reduced by Li+, and this was coupled with reductions in citrate synthase and endogenous anaplerotic absolute fluxes, although no significant changes in the

relative anaplerotic flux (y) were detected in the presence of Li^+. This suggests a direct inhibitory effect of Li^+ on TCA cycle flux. Possible inhibition sites of the TCA cycle by Li^+ could include aconitase (Abreu & Abreu, 1973). ^{13}C NMR spectra revealed a tendency for higher levels of ^{13}C-enriched citrate in the presence of Li^+, which is consistent with accumulation of citrate as a result of decreased aconitase activity. Moreover, increased citrate levels would inhibit key regulatory glycolytic enzymes such as phosphofructokinase thus contributing to the reduction in glucose conversion into pyruvate.

To determine if Li^+ has an effect on the competition between glucose and lactate oxidation when both substrates are available, the contribution of exogenous 5 mmol L^{-1} [U-^{13}C]glucose and 5 mmol L^{-1} [3-^{13}C]lactate to the TCA cycle acetyl-CoA pool was quantified by ^{13}C-isotopomer analysis in the absence and presence of Li^+ (Figure 7B). Both initial glucose and lactate concentrations were higher than the apparent K_m for glucose and lactate transporters, 1.16 mmol L^{-1} (Lust et al., 1975) and 1 mmol L^{-1} (Dringen et al., 1995), respectively; therefore, transport was not expected to be rate limiting for either substrate. Relative fluxes corresponding to the fraction of acetyl-CoA derived from [U-^{13}C]glucose (lac_{123}), [3-^{13}C]lactate (lac_3), and unlabelled endogenous sources (fat_0) are shown in Table 3.

Relative Flux Parameter	Control	1 mmol L^{-1} Li^+	15 mmol L^{-1} Li^+
Acetyl-CoA from [U-^{13}C]glucose (lac_{123})	0.26 ± 0.03 (n=3)	0.26 ± 0.03 (n=3)	0.26 ± 0.03 (n=3)
Acetyl-CoA from [3-^{13}C]lactate (lac_3)	0.62 ± 0.03 (n=3)	0.63 ± 0.03 (n=3)	0.65 ± 0.03 (n=3)
Acetyl-CoA from endogenous sources (fat_0)	0.12 ± 0.01 (n=3)	0.12 ± 0.03 (n=3)	0.10 ± 0.03 (n=3)
Endogenous anaplerotic flux (y)	0.20 ± 0.02 (n=3)	0.19 ± 0.02 (n=3)	0.15 ± 0.02 * (n=3)

Table 3. Relative metabolic fluxes for SH-SY5Y cells incubated for 24 h at 37 °C in KRB medium containing a mixture of 5 mmol L^{-1} [U-^{13}C]glucose and 5 mmol L^{-1} [3-^{13}C]lactate, in the absence (control) and presence of 1 or 15 mmol L^{-1} Li^+ (Fonseca et al., 2005). Values are average $\pm$ SD for the number (n) of experiments indicated in parentheses. All fluxes are relative to a citrate synthase flux of 1.0 . * $p < 0.05$, relative to control.

In control cells, over 60% of the acetyl-CoA was derived from [3-^{13}C]lactate, more than twice the contribution from [U-^{13}C]glucose, demonstrating that exogenous lactate is highly preferred over glucose for TCA cycle oxidation under these conditions. The presence of either 1 or 15 mmol L^{-1} Li^+ did not alter the relative utilisation of exogenous lactate and glucose. However, 15 mmol L^{-1} Li^+ resulted in a small but significant reduction in anaplerotic flux from endogenous sources.

3.1.2 Li^+ effects on the metabolic balances in cortical astrocytes and neurons

The metabolic balance between glucose or acetate consumption and lactate production by primary cultures of rat cortical astrocytes and neurons incubated with a mixture of 5 mmol L^{-1} glucose and 5 mmol L^{-1} acetate or with 1 mmol L^{-1} glucose, respectively, in the absence (control) and presence of 1 or 15 mmol L^{-1} Li^+, was evaluated by classical enzymatic assays. Table 4 shows the glucose or acetate consumption as well as lactate production rates

calculated for cortical astrocytes and neurons, in the absence (control) and presence of two Li$^+$ concentrations.

Cell type	Metabolic rates (mmol L^{-1} h^{-1} mg^{-1})	Control	1 mmol L^{-1} Li$^+$	15 mmol L^{-1} Li$^+$
Astrocytes	Glucose consumption	3.19 ± 0.19 (n=5)	2.83 ± 0.27 (n=7)	3.46 ± 0.33 (n=5)
	Acetate consumption	1.37 ± 0.67 (n=5)	1.11 ± 0.11 (n=5)	1.24 ± 0.52 (n=4)
	Lactate production	4.02 ± 0.12 (n=5)	3.94 ± 0.14 (n=7)	4.48 ± 0.35 (n=6)
Neurons	Glucose consumption	2.50 ± 0.07 (n=6)	2.34 ± 0.11 (n=6)	2.22 ± 0.10 * (n=6)
	Lactate production	0.43 ± 0.08 (n=5)	0.48 ± 0.10 (n=5)	0.37 ± 0.04 (n=5)

Table 4. Glucose consumption and lactate production rates by cortical astrocytes or neurons incubated in the absence (control) and presence of 1 or 15 mmol L^{-1} Li$^+$. Acetate consumption rates by astrocytes under control and Li$^+$ conditions are also shown. Astrocytes were incubated in KRB medium containing a mixture of 5 mmol L^{-1} glucose and 5 mmol L^{-1} acetate, while neurons were incubated with 1 mmol L^{-1} glucose. Glucose and acetate consumption as well as lactate production were defined as the difference between the extracellular concentrations at the different time points (t) and the initial concentrations (at t = 0 h), i.e., ([glucose]t - [glucose]t=0h), ([acetate]t - [acetate]t=0h) and ([lactate]t - [lactate]t=0h), respectively (Fonseca et al., 2009). Values are means ± SEM for the number (n) of experiments indicated in parentheses. * p < 0.05 relative to control.

As expected, neurons showed a preferential oxidative metabolism with a relatively modest lactate production, since only 9 % of the glucose consumed was converted into lactate, while 91 % was oxidised in the neuronal TCA cycle. In contrast, astrocytes were found to be more glycolytic as approximately 63 % of the glucose consumed by astrocytes was converted into lactate, while only 37 % was oxidised in the astrocytic TCA cycle (Hassel et al., 1995). Our results revealed that 15 mmol L^{-1} Li$^+$ caused a statistically significant decrease in glucose uptake by neurons but no apparent effects in glucose or acetate uptake by astrocytes. The decrease in neuronal glucose uptake in the presence of Li$^+$, consistent with an inhibition of the glycolytic flux, was not paralleled by a concomitant significant change in lactate production, indicating that the decreased glucose consumption reflects a net decrease in glucose oxidation and TCA cycle activity (Fonseca et al., 2009). The ability of Li$^+$ to decrease glycolytic and TCA cycle fluxes is in agreement with the results obtained for SH-SY5Y cells (Fonseca et al., 2005) and other data in the literature (Abreu & Abreu, 1973; Kajda & Birch, 1981; Nordenberg et al., 1982).

In summary, the present study provides evidence that both TCA cycle and glycolysis are targets for Li$^+$ action in the neuroblastoma SH-SY5Y cell line and the inhibition of the TCA cycle, and hence of cell energy production, observed for therapeutic concentration of Li$^+$ (1 mmol L^{-1}) may constitute one hypothesis for the mechanism by which Li$^+$ exerts its antimanic effect. However, in cortical neurons only the highest Li$^+$ concentration (15 mmol

L-1) was able to decrease neuronal glucose consumption and TCA cycle activity. Although Li+ has a narrow therapeutic range—it is toxic *in vivo* for plasma concentrations higher than 2 mmol L-1 —the 15 mmol L-1 Li+ concentration was found to be nontoxic for both neurons and astrocytes under our experimental conditions (data not shown). Furthermore, Li+ concentrations achieved in the intercellular space are uncertain, but are expected to reach much higher levels than in plasma. Despite these limitations, the results presented here strengthen the importance of cell energetic metabolism as a target for Li+ action, an area of study that has been underestimated and poorly reported in the literature.

3.2 Li+ effects on glutamatergic and GABAergic neurotransmissions in adult rat brain and cultured brain cells, as revealed by ^{13}C NMR

Besides its metabolic effects, Li+ was proposed to alter the balance between excitatory and inhibitory neurotransmitter systems, thus modulating glutamatergic and GABAergic neurotransmission (Antonelli et al., 2000; Brambilla et al., 2003; Gottesfeld, 1976; Jope et al. 1989; Marcus et al., 1986; O'Donnell et al., 2003; Otero Losada & Rubio, 1986; Petty, 1995; Rubio & Otero Losada, 1986; Shiah & Yatham, 1998) and facilitating in this way, mood recovery and stabilisation in Li+-treated bipolar patients. However, the effects of Li+ have been studied using different experimental models and protocols that have often yielded different or even contradictory results. In this study, we have used the ^{13}C NMR technique to investigate the effects of Li+ on the metabolism of glutamate, glutamine and GABA in the adult intact rodent brain and in primary cultures of cortical neurons and astrocytes. This technique has been used successfully to study cerebral metabolic compartmentation and the glutamate-glutamine cycle as the basis of glutamatergic and GABAergic neurotransmissions (Rodrigues & Cerdán, 2005).

Adult male rats receiving a single dose of Li+ intraperitoneally (7 mmol kg-1), or saline (control), were infused with [1-^{13}C]glucose or [2-^{13}C]acetate. Glucose is considered a universal substrate for neurons and glial cells, although it is thought to be metabolized more in the neuronal TCA cycle; in contrast, acetate is considered a glial substrate because it is selectively taken up by astrocytes by a specialized transport system, which is absent or less active in neurons (Waniewski & Martin, 1998; Sonnewald & Kondziella, 2003). Brain extracts were prepared 3 h after Li+ injection and analysed by ^{13}C NMR. The mean Li+ concentrations in brain and plasma achieved 3 h after i.p. Li+ injection were 1.5 ± 0.4 mmol kg-1 tissue wet-weight (n=5) and 1.3 ± 0.5 mmol L-1 (n=7), respectively. Figure 9 summarizes the results obtained from the quantitative analysis of ^{13}C incorporation in the aliphatic carbons of glutamate, glutamine and GABA from the brain of control and Li+-treated animals.

With [1-^{13}C]glucose as substrate, Li+ decreased the incorporation of ^{13}C in the observable carbons of glutamate, glutamine and GABA, with statistical significance for the C4 and C3 carbons of glutamate and GABA, respectively. Apparently Li+ administration did not change the ^{13}C labelling of these metabolites after [2-^{13}C]acetate infusions. Because [1-^{13}C]glucose is believed to be a universal substrate for neurons and glial cells and [2-^{13}C]acetate is known to be mainly a glial substrate, our results suggest that the inhibition observed *in vivo* must occur primarily in the neuronal compartment, at an upstream level of the glutamate-glutamine-GABA cycles. Glucose consumption through glycolysis and the TCA cycle could be a possible target for this upstream Li+ action (Fonseca et al., 2005, 2009;

Nordenberg et al., 1982; Plenge, 1976; Zager & Ames, 1988;). Li+ significantly increased the glutamate C3/GABA C3 labelling ratio (p < 0.01), suggesting that Li+ may affect the synthesis of GABA from its direct precursor glutamate in the neuronal compartment, *in vivo*, possibly through the inhibition of glutamate decarboxylase activity (Fonseca et al., 2009).
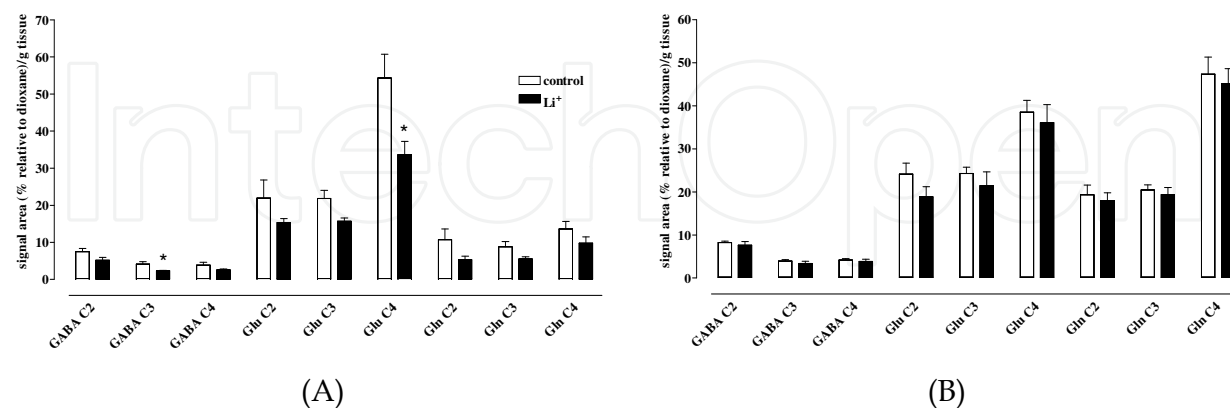

Fig. 9. Graphical representation of 13C NMR signal areas of the metabolites glutamate, glutamine and GABA, as observed in the 13C NMR spectra obtained form rat brain extracts prepared after saline (control) and Li+ administration, and infusion with [1-13C]glucose (n=3 for both saline- and Li+-treated rats) (**A**) or [2-13C]acetate (n=4 for saline- and n=5 for Li+-treated rats) (**B**) (Fonseca et al., 2009). Tissue wet weight and appropriate correction factor for nuclear Overhauser enhancement and signal saturation were taken into account. Values are means ± SEM for the indicated number of experiments. * p < 0.05 relative to control. Glu - glutamate; Gln – glutamine.

To investigate this mechanism in more detail, we used primary cultures of cortical neurons and astrocytes. The 13C NMR spectra of extracts obtained from the cellular layers of astrocyte cultures after incubation with 5 mmol L^{-1} [2-13C]acetate, or neuron cultures incubated with 1 mmol L^{-1} [U-13C]glucose, showed an extensive incorporation of 13C from the 13C-labeled substrates in the C2, C3, and C4 carbons of glutamate and glutamine, C2 and C3 of aspartate (and C2, C3, and C4 of GABA and C3 of lactate for neurons). Table 5 shows the relative ratios between the areas of the C4 and C3 carbon resonances of glutamine and glutamate obtained from the 13C NMR spectra of astrocyte extracts, as well as the ratios between the areas of the C2, C3, and C4 carbon resonances of glutamate and the C4, C3 and C2 carbon resonances of GABA, respectively, obtained from the 13C NMR spectra of neuron extracts. The reason for selecting and comparing the areas of these specific carbon resonances of glutamate and GABA was based on the well-known metabolic fate of 13C labelling from 13C-labeled substrates because the order of 13C-labeled carbons in glutamate is reversed in GABA (e.g., the labels in (2(4)-13C) glutamate end up subsequently in (4(2)-13C) GABA) (Sonnewald & Kondziella, 2003).

When 15 mmol L^{-1} was used, an increase in glutamate C2/GABA C4 (p<0.05), glutamate C3/GABA C3 and glutamate C4/GABA C2 13C labelling ratios was observed, suggesting that Li+ may decrease GABA synthesis from glutamate, its direct precursor in cortical GABAergic neurons. These findings reflect a direct inhibitory effect of Li+ on glutamate decarboxylase activity and are in agreement with the in vivo studies, where a more pronounced reduction in 13C labelling of GABA relative to glutamate was observed. Indeed,

previous studies have reported Li$^+$-induced inhibitory effects on glutamate decarboxylase (Otero Losada & Rubio, 1986; Rubio & Otero Losada, 1986).

Cell type	Area ratio	Control	1 mM Li$^+$	15 mM Li$^+$
Astrocytes	Gln C4/Glu C4	0.76 ± 0.37	0.58 ± 0.29	0.32 ± 0.17
	Gln C3/Glu C3	1.12 ± 0.54	1.13 ± 0.43	0.64 ± 0.29
Neurons	Glu C2/GABA C4	1.60 ± 0.15	1.64 ± 0.21	2.95 ± 0.45 *
	Glu C3/GABA C3	2.12 ± 0.26	1.69 ± 0.29	3.64 ± 1.06
	Glu C4/GABA C2	2.04 ± 0.19	1.99 ± 0.35	3.12 ± 0.79

Table 5. Relative ratios between the areas of the C4 and C3 carbon resonances of glutamine (Gln) and glutamate (Glu), as well as between the areas of the C2, C3 and C4 carbon resonances of GABA and the C4, C3 and C2 carbons of Glu, respectively, calculated from the ^{13}C NMR spectra of astrocyte or neuron extracts. Cells were incubated for 24 h at 37 $^{\circ}$C in the absence (control) and presence of 1 and 15 mmol L^{-1} Li$^+$, in a modified KRB medium containing 5 mM [2-^{13}C]acetate (astrocytes) or 1 mM [U-^{13}C]glucose (neurons) (Fonseca et al., 2009). Values are means ± SEM of 3 independent experiments. * p < 0.05, relative to the control.

In summary, Li$^+$ was found to decrease the incorporation of ^{13}C labelling into GABA carbons from its precursor glutamate in neurons, both ex vivo and in vivo, probably through the inhibition of glutamate decarboxylase. These inhibitory effects, together with those detected in glucose consumption and TCA cycle activity of neurons, configure a complex mechanism of Li$^+$ action involving inhibitory actions at multiple sites. The results presented here may provide a new insight into the basis of the metabolic effects of Li$^+$ on brain metabolism involving the modulation of the main excitatory and inhibitory systems, which may facilitate mood recovery and stabilization in bipolar patients.

4. Effect of mood stabilizers on the regulation of cyclic AMP levels by dopaminergic and β-adrenergic receptors

4.1 Intracellular lithium and cyclic AMP levels are mutually regulated in neuronal cells

Recent research has been focused on how Li$^+$ changes the activity of cellular signal transduction systems, in particular those involving AC. It has been suggested that cAMP levels are abnormal in bipolar patients and are regulated by mood stabilizing agents. So, it is important to know whether this second messenger regulates Li$^+$ transport into neuronal cells and determine the effect of Li$^+$ on the homeostasis of intracellular cAMP levels, which depends on the AC activity. Thus, the effect of intracellular cAMP on Li$^+$ uptake, at therapeutic plasma concentrations, in SH-SY5Y human neuroblastoma cells and in primary cultures of rat cortical and hippocampal neurons was studied. The cells were stimulated with forskolin, a direct activator of the catalytic subunit of AC, or with the cAMP analogue dibutyryl-cAMP, to increase intracellular cAMP levels. Intracellular Li$^+$ was quantified by AA spectrophotometry and cAMP levels were determined under basal and forskolin stimulated-conditions, and in the presence and absence of Li$^+$, through a radioactive assay using [8-^{3}H]cAMP.

The kinetics of Li^{+} influx and Li^{+} uptake by SH-SY5Y cells and cortical and hippocampal neurons, in the presence and absence of forskolin, was studied and the results presented in Figure 10 details of experimental procedure in figure legend).

It was observed (Figure 10 A,B) that under forskolin stimulation both the Li^{+} influx rate constant k_i, [0.028 ± 0.005 min^{-1} (ctrl) and 0.041 ± 0.005 min^{-1} (fsk); $p < 0.05$] and the Li^{+} accumulation in SH-SY5Y cells were increased (27.6 ± 1.8 nmoL mL^{-1} vs the control value 17.9 ± 1.7 nmoL mL^{-1}; $p < 0.01$). Dibutyryl-cAMP also increased Li^{+} uptake confirming that these effects were due to an increase in intracellular cAMP and not to a non-specific effect of forskolin [126.9 ± 11.6 % for forskolin ($p < 0.01$ relative to ctr) and 142.6 ± 13.9 % for db-cAMP ($p < 0.001$, relative to ctr) and not significantly different between them]. Identical results were obtained with cortical [133.5 ± 5.9 % for forskolin ($p < 0.01$) and 154.0 ± 9.3 % for db-cAMP ($p < 0.001$)] and hippocampal neurons [133.3 ± 11.9 % for forskolin ($p < 0.05$) and 141.4 ± 6.9 %; for db-cAMP ($p < 0.05$)] (Figure 10 C,D). To obtain information about the transport pathways responsible for Li^{+} uptake under resting and forskolin stimulated conditions, experiments were carried out using inhibitors of specific transporters at SH-SY5Y cells membrane (details are in the legend of the figure) and the intracellular Ca^{2+} chelator BAPTA. The graphs of Figure 11 show the data obtained.

(A)   (B)   (C)   (D)
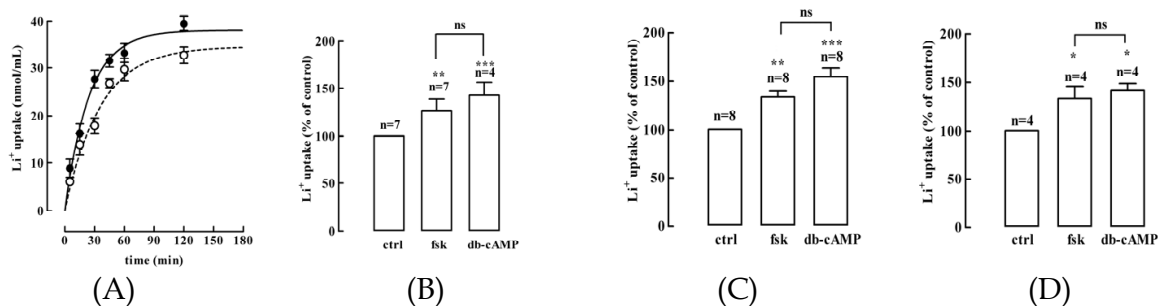
Fig. 10. Kinetics of Li^{+} influx in SH-SY5Y cells, in the absence (○) (ctrl) and in the presence (●) of forskolin (fsk) **(A)**. The cells were pre-incubated with RO-201724, the cAMP phosphodiesterase inhibitor (Miles et al., 1987), (25 μmol L^{-1}), for 15 min, and then with fsk (10 μmol L^{-1}), for 15 min. LiCl at 1 mmol L^{-1} concentration was then added to the medium and at 5, 15, 30, 45, 60 or 120 min; the amount of Li^{+} taken up by cells was measured by AA spectrophotometry. The rate constants obtained for Li^{+} influx were 0.028 ± 0.005 min^{-1} (ctrl) and 0.041 ± 0.005 min^{-1} (fsk) ($p < 0.05$). Values are means $\pm$ SEM of 4-20 independent experiments. Li^{+} uptake by SH-SY 5Y cells **(B)**, by cortical **(C)** or hippocampal neurons **(D)**, pre-treated or not (ctrl) with fsk (10 μmol L^{-1}; 15 min) or db-cAMP (500 μmol L^{-1}; 30 min) after pre-incubating the cells with RO-201724 (25 μmol L^{-1}, 15 min), and before incubation with 1 mmol L^{-1} Li^{+}, for 30 min. The total amount of intracellular Li^{+} was measured by AA spectrophotometry, as described in (Montezinho et al., 2004). Data are presented as a percentage of intracellular Li^{+} content relative to the control. Values are means $\pm$ SEM., for the indicated number of independent experiments. *, $p < 0.05$; **, $p < 0.01$; ***, $p < 0.001$, significantly different from control; ns= not significant (Montezinho et al., 2004).
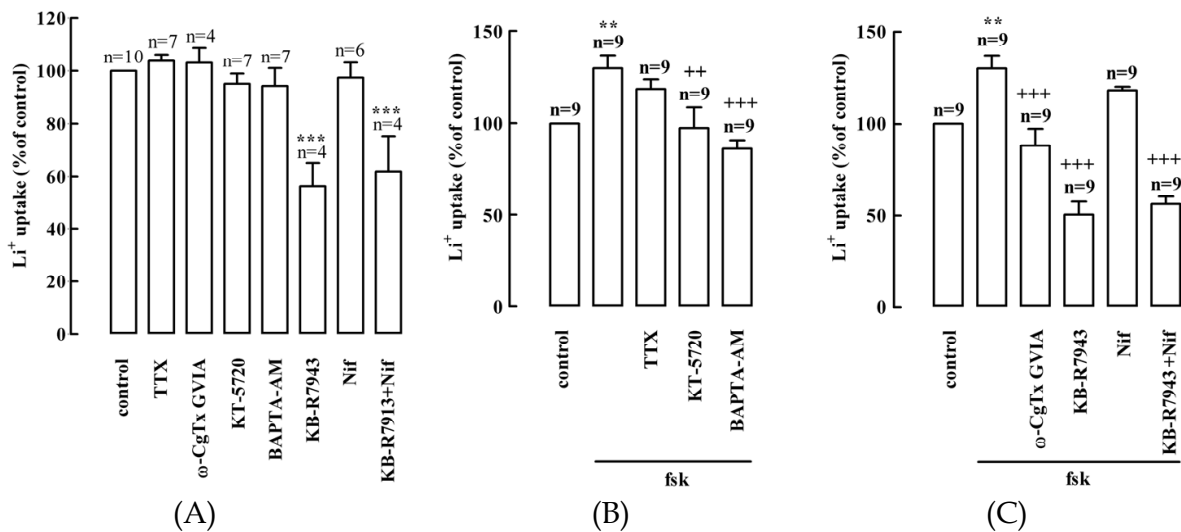
Fig. 11. Pharmacological characterization of Li^+ uptake by SH-SY5Y cells under resting conditions (**A**) and after fsk stimulation (**B**) and (**C**). The cells were pre-treated with RO-201274 (25 μmol L^{-1}, 15 min), and then with the following drugs, at different concentrations and pre-incubation times: TTX (1 μmol L^{-1}; 5 min), ω-Conotoxin GVIA (ω-CgTx GVIA;0.5 μmol L^{-1}; 30 min), KT-5720 (10 μmol L^{-1}; 10 min), BAPTA-AM (10 μmol L^{-1}; 30 min), KB-R7943 (20 μmol L^{-1}; 5 min) and nifendipine (Nif) (1 μmol L^{-1}; 5 min), to study the contribution of voltage-sensitive sodium channels (VSSC), N-type voltage-sensitive calcium channels (VSCC), PKA, $[Ca^{2+}]_i$, Na^+/Ca^{2+} exchanger and L-type VSCC, respectively, for Li^+ uptake by the cells under resting conditions (**A**). To study the contribution of all these transport pathways to the fsk-induced Li^+ uptake, after exposure to the drugs, in the same concentrations and pre-incubation times, the cells were incubated with fsk (10 μmol L^{-1}), for 15 min (B, C). Then, in all cases, 1 mmol L^{-1} LiCl was added to the medium and after 30 min the amount of Li^+ taken up by the cells was measured by AA spectrophotometry. Total intracellular Li^+ content is presented as a percentage relative to the control. Values are means ± SEM, for the indicated number of independent experiments. ***, $p< 0.01$ and **, $p< 0.01$, significantly different from control, respectively, under resting and fsk stimulated conditions; +, $p< 0.05$; ++, $p< 0.01$; +++, $p< 0.001$, significantly different from fsk stimulation in the absence of any of these drugs (Montezinho et al., 2004).

Under resting conditions, the inhibitor of the Na^+/Ca^{2+} exchanger, KB-R7943, reduced the influx of Li^+ and completely inhibited the effect of forskolin on the increase of Li^+ uptake, although this effect was attenuated also by KT-5720 (protein kinase A (PKA) inhibitor), ω-Conotoxin GVIA (N-type voltage-sensitive calcium channels (VSCC) inhibitor) or BAPTA (Ca^{2+} chelator). This indicates that the Na^+/Ca^{2+} exchanger is the principal responsible for Li^+ influx into SH-SY5Y cells in these conditions.

The involvement of intracellular Ca^{2+} concentration ($[Ca^{2+}]_i$) in Li^+ uptake, under resting and after forskolin stimulation, was investigated in the presence of different inhibitors of pathways which contribute to $[Ca^{2+}]_i$ homeostasis by measuring intracellular free Ca^{2+} levels using fluorescence spectroscopy (Figure 12).
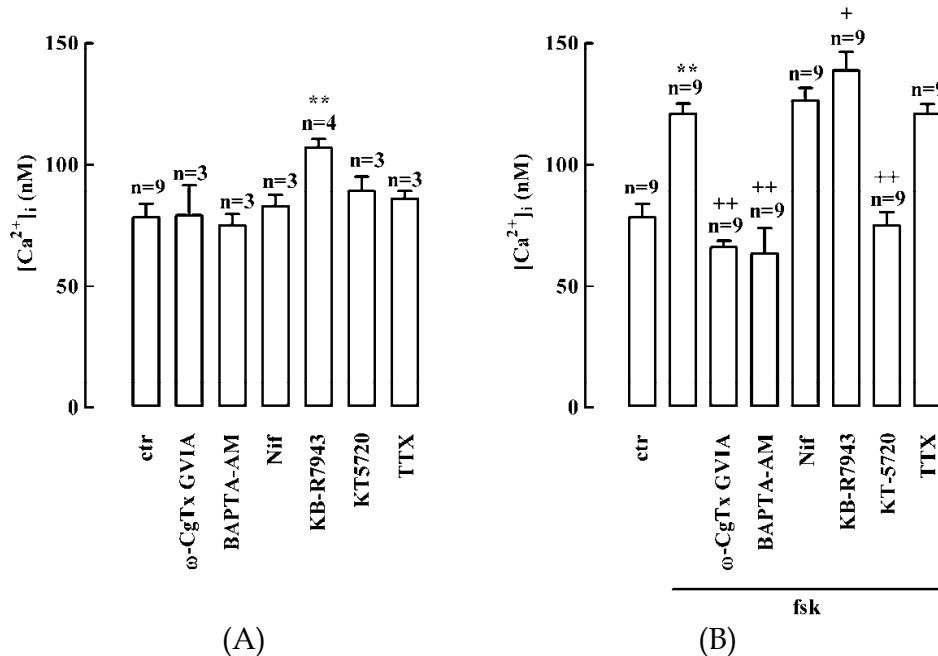
Fig. 12. Pharmacological characterization of the pathways for [Ca2+]i homeostasis in SH-SY5Y cells under resting conditions **(A)** and after stimulation with fsk **(B)**. Cells were pre-treated with RO-201724 (25 μmol L^{-1},15 min), and then with ω-CgTx GVIA (0.5 μmol L^{-1}; 30 min), Nif (1 μmol L^{-1}; 5 min), KB-R7943 (20 μmol L^{-1}; 5 min), KT-5720 (10 μmol L^{-1}; 10 min) or TTX (1 μmol L^{-1}; 5 min), to test the contribution of N- and L-type VSCC, Na$^+$/Ca^{2+} exchanger, PKA and VSSC, respectively, to the maintenance of the [Ca^{2+}]$_i$. The effect of the Ca^{2+} chelator, BAPTA, was also determined by pre-incubating the cells with 10 μmol L^{-1} BAPTA-AM, for 30 min. The cells were stimulated or not with 10 μmol L^{-1} fsk, for 15 min, and the [Ca^{2+}]$_i$ was determined by fluorescence spectroscopy using fura-2. Values are means ± SEM, for the indicated number of independent experiments. **, p< 0.01, significantly different from control; +, p< 0.05; ++, p< 0.01, significantly different from fsk stimulation in the absence of any drug (Montezinho et al., 2004).

It was observed that under resting conditions only KB-R7943 increased [Ca^{2+}]$_i$ in SH-SY5Y cells, confirming the role of the Na$^+$/Ca^{2+} exchanger on intracellular homeostasis (Figure 12A). Intracellular Ca^{2+} chelation (with BAPTA), or inhibition of N-type VSCC (ω-CgTx GVIA), or inhibition of cAMP-dependent protein kinase A (KT-5720) abolished the effect of forskolin on Li$^+$ uptake (Figure 12B). All these conditions decrease free [Ca^{2+}]$_i$, as demonstrated by the quantification of Ca^{2+} levels, demonstrating the involvement of Ca^{2+} on forskolin-induced Li$^+$ uptake.

SH-SY5Y cells were exposed to 1 mmol L^{-1} Li$^+$ for different periods of time to check its effect on cAMP levels. Figure 13A shows that after 24 h to Li$^+$ exposure, basal cAMP levels increased, which can be explained by the inhibition of G$_i$, the G proteins most active in basal conditions. Pre-incubation of the cells with 1 mmol L^{-1} Li$^+$, during 1, 24 or 48 h, decreased cAMP production in response to forskolin (Figure 13B) which may be due to inhibition of AC activity as a result from Li$^+$/Mg^{2+} competition.

(A)   (B)   (C)
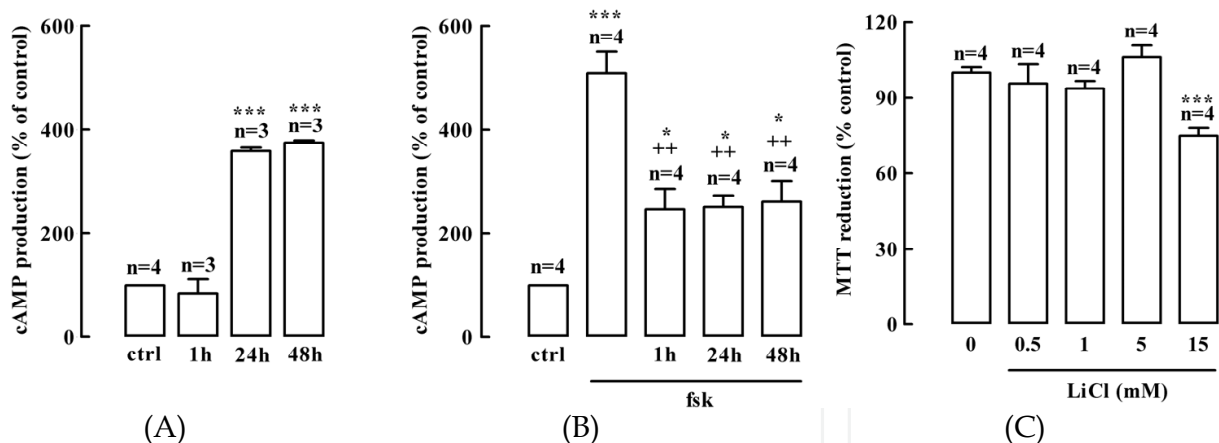
Fig. 13. Effects of Li^+ on cAMP production by SH-SY5Y cells. **(A)** Cells were pre-treated with RO-201724 (25 μmol L^{-1}, 15 min), and then incubated or not (ctrl) with 1 mmol L^{-1} Li^+, for the indicated periods of time. **(B)** Where indicated, the cells were stimulated with 10 μmol L^{-1} fsk, for 15 min, after treatment with Li^+. The cAMP levels were measured as described (Montezinho et al., 2004). **(C)** MTT biochemical assay with SH-SY5Y cells treated with LiCl (0, 0.5, 1, 5 and 15 mmol L^{-1}), during a period of 48h. Data are presented as a percentage relative to the control. Values are means $\pm$ SEM, for the indicated number of independent experiments. *, p< 0.05; ***, p< 0.001, significantly different from the control. $^{++}$, p< 0.01, significantly different from fsk stimulation in the absence of Li^+ (Montezinho et al., 2004).

These data indicate that forskolin AC activation increases Li^+ influx in the three cellular models, an effect mediated by PKA and due to changes in $[Ca^{2+}]_i$. The intracellular cAMP accumulation increases $[Ca^{2+}]_i$, due to its entry through N-type VSCC, thus activating Na^+/Ca^{2+} exchanger allowing the increase of Li^+ influx, by substituting Na^+, in exchange with Ca^{2+} extrusion (Deval et al., 2002; Fonseca et al., 2004; Montezinho et al., 2004).

Overall, these results demonstrate that intracellular cAMP levels regulate Li^+ uptake in a Ca^{2+}-dependent manner, and Li^+ plays an important role in the homeostasis of this second messenger in neuronal cells. This is relevant data to understand the mechanism of action of Li^+, taking into account several aspects already mentioned in the literature such as: bipolar disorder is associated with deregulation in AC mediated signal transduction processes, which are affected by Li^+ (Berns & Nemeroff, 2003; Brunello & Tascedda, 2003; Manji & Lenox, 2000a, 2000b; Manji et al., 2001), and with increased $[Ca^{2+}]_i$ (Hough et al., 1999) pointing to an interaction between intracellular signalling mechanisms mediated by Ca^{2+} and cAMP (Cooper et al., 1995); bipolar patients with a $[Ca^{2+}]_i$ higher than normal respond better to Li^+ treatment, indicating a possible correlation between Ca^{2+} levels and Li^+ response (Ikeda & Kato, 2003).

4.2 Effect of mood stabilizers on dopamine D_2-like receptor-mediated inhibition of adenylate cyclase

Second messenger-mediated pathways represent targets for Li^+ action; thus, it is important to investigate whether other mood stabilizing agents exert similar effects on the same signalling pathways. Bipolar disorder seems to be associated with an enhanced signalling activity of the cAMP cascade and most of its events have been implicated in the action of

mood stabilizing drugs, which somehow modulate brain cAMP levels. Therefore, the effects of Li⁺, carbamazepine and valproate on basal and forskolin-evoked cAMP accumulation were studied both ex vivo, in cultured cortical neurons, and in vivo in the rat prefrontal cortex using microdialysis in freely moving animals, a technique which detects extracellular cAMP levels, thus accurately reflecting intracellular changes in AC activity (Masana et al., 1991, 1992). It has been demonstrated that a fraction of intracellular cAMP generated by activation of AC is extruded into the extracellular fluid in proportion with its accumulation in cells. Therefore, the efflux of cAMP can be used to study the cAMP second messenger system in intact brains, using in vivo microdialysis (Mørk & Geisler, 1994). Moreover, the capacity of dopamine D_2-like receptors stimulation, with quinpirole, to block the increase of forskolin-stimulated cAMP levels was measured under control conditions and after treatment with the mood stabilizing drugs. The cAMP was quantified using the [8-³H] and [¹²⁵I] radioimmunoassay kits, respectively for the ex vivo and in vivo experiments.

Figure 14 shows the determination of intracellular cAMP levels in cultured cortical neurons as a response to different experimental conditions (protocols are detailed in the figure legend).
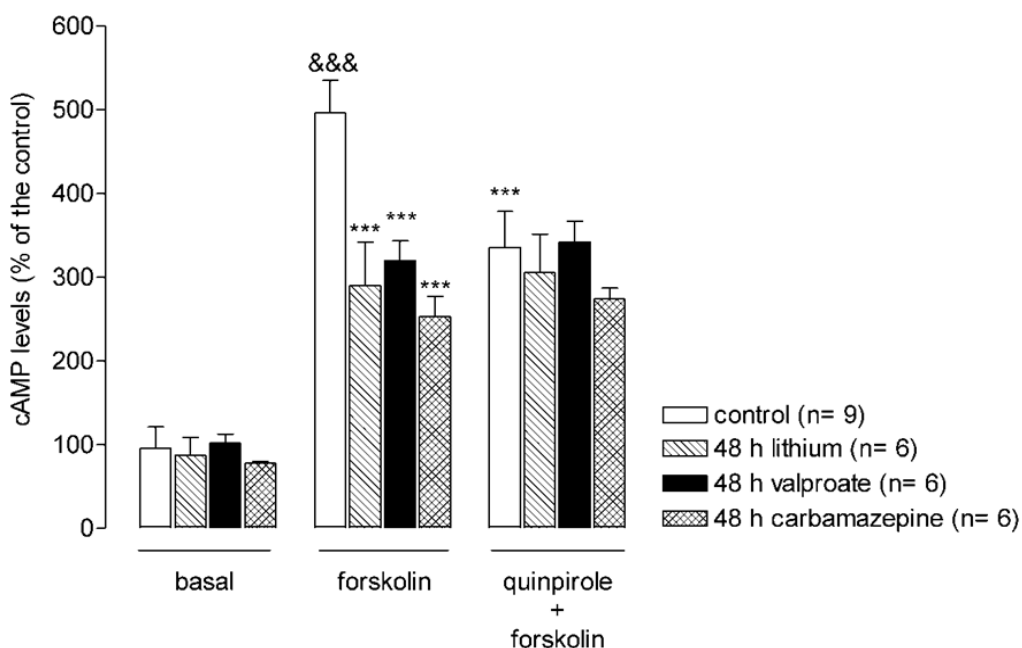
Fig. 14. Effects of lithium, valproate and carbamazepine on the intracellular cAMP levels in cultured cortical neurons under basal conditions and after stimulation with forskolin or quinpirole plus forskolin. Neurons were pre-exposed or not (control) to 1 mmol L⁻¹ lithium, 0.05 mmol L⁻¹ carbamazepine or 0.5 mmol L⁻¹ valproate, for 48 h. After this period, neurons were incubated with Ro-201724 (25 μmol L⁻¹; 15 min) and were then treated or not (basal) with forskolin (10 μmol L⁻¹; 15 min), or with forskolin together with quinpirole (10 μmol L⁻¹; 15 min). In the latter experimental conditions the cells were pre-treated with 10 μmol L⁻¹ quinpirole for 5 min. The cAMP levels were measured as described (Montezinho et al., 2007). The levels of cAMP are presented as percentage relative to the control. Data are means ± SEM, for the indicated number of independent experiments, performed in duplicate. Data were analysed by one-way ANOVA, followed by post-hoc Bonferroni´s test. &&&, p< 0.001 compared to control untreated cells; ***, p< 0.01 compared to control forskolin-stimulated cells (Montezinho et al., 2007).

Lithium, carbamazepine or valproate had no effect on the basal cAMP production, but partially inhibited forskolin-induced cAMP accumulation (control: 495.8 ± 39.0 %, p < 0.001 (5× basal value); lithium: 290.1 ± 51.8 %, p< 0.001; carbamazepine: 273.9 ± 13.1 %, p< 0.001; valproate: 319.6 ± 23.4 %, p< 0.001). In the presence of quinpirole, the agonist of dopamine D_2-like receptors, no effect on the basal cAMP accumulation was observed (data not shown), but inhibition of forskolin-enhanced cAMP levels occurred in untreated neurons (335.6 ± 42.8 %, p< 0.001); the activation of dopamine D_2-like receptors had no additional effect in cortical neurons treated with the mood stabilizers (lithium: 305.2 ± 46.2 %; carbamazepine: 273.9 ± 13.1 %; valproate: 341.9 ± 24.7 %, p< 0.001).

Similar experiments were carried out *in vivo*. Extracellular cAMP levels were determined in prefrontal cortex of freely moving rats by microdialysis and the obtained results are shown in Figure 15 (detailed experimental conditions are in the legend of this figure).

(A)   (B)
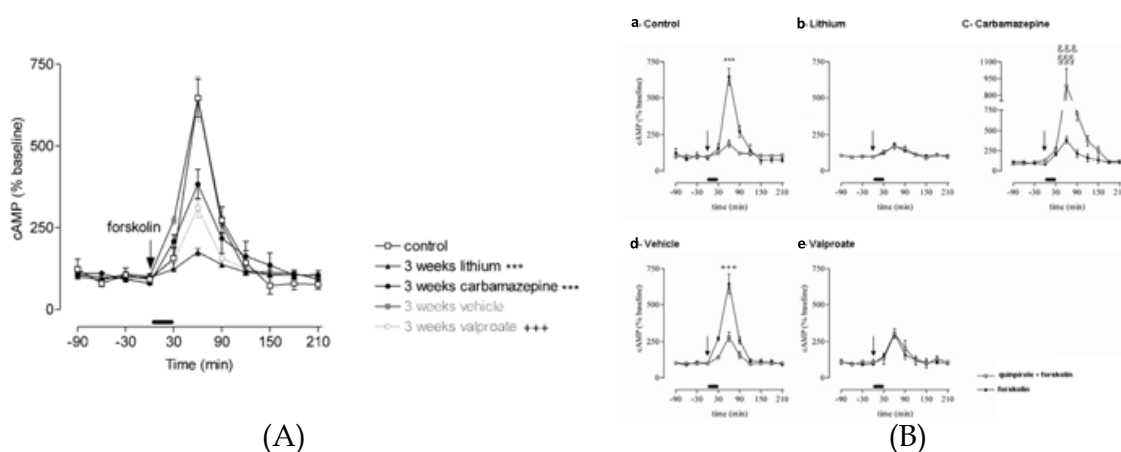
Fig. 15. Effect of local infusion of forskolin (100 µmol L^{-1}) **(A)** and forskolin (100 µmol L^{-1}) or quinpirole (100 µmol L^{-1}) simultaneously with forskolin (100 µmol L^{-1}) **(B)** in the prefrontal cortex of freely moving rats (starting at arrow and maintained during 30 min) on the extracellular cAMP levels of **(A)** control-, vehicle-, lithium-, valproate- or carbamazepine-treated rats; **(B)** control rats **a)** or rats chronically treated with lithium **b),** carbamazepine **c),** vehicle **d)** or valproate **e).** Baseline levels of cAMP were taken as the average cAMP content in the four consecutive samples collected 3 h after the insertion of the probe. Thereafter, the agent of interest (100 µmol L^{-1} forskolin or 100 µmol L^{-1} quinpirole plus 100 µmol L^{-1} forskolin) dissolved in Ringer solution was infused through the probe, for 60 min, and seven samples were then collected. Extracellular cAMP levels in the dialysates were measured by radioimmunoassay analysis and expressed as percentage of the basal value. Results are expressed as means ± SEM, from 4 to 6 independent experiments. The rats were treated or not, during three weeks, with therapeutic doses of lithium (n= 6) or carbamazepine (n=6) in the diet, whereas others were treated with therapeutic doses of valproate (n= 6) by intraperitoneal injections once daily, for three weeks. Control rats (n= 6) received standard diet, whereas vehicle rats (n= 4) received intraperitoneal injections with saline solution (NaCl 0.9%) once daily during three weeks (Montezinho et al., 2007). Data are analyzed by one-way ANOVA, followed by post-hoc Bonferroni´s test. ***, p< 0.001; compared to the cAMP produced 60 min after the infusion of forskolin in control rats. $^{+++}$, p< 0.001; compared to the cAMP produced 60 min after the infusion of forskolin in vehicle-treated rats. §§§, p< 0.001; compared to the cAMP produced 60 min after the infusion of quinpirole plus forskolin in control rats. $^{\&\&\&}$, p< 0.001, compared to the cAMP produced 60 min after the infusion of forskolin in carbamazepine-treated rats.

After forskolin infusion in the prefrontal cortex of the rats, for 30 min, the average basal cAMP levels (control: 9.68 ± 2.10 fmoL/20 μL; lithium-treated animals: 13.17 ± 1.21 fmoL/20 μL ($p< 0.05$ relative to control); carbamazepine-treated rats, 7.82 ± 0.34 fmoL/20 μL ($p< 0.01$ relative to control); valproate-treated rats: 10.42 ± 1.06 fmoL/20 μL) increased to approximately 647.0 ± 58.3 % and 644.5 ± 68.9 % of the basal values (control and vehicle, respectively) whereas in lithium-, carbamazepine- or valproate-treated rats there was a statistically significant decrease in the forskolin-stimulated cAMP levels determined after 60 min of forskolin infusion (lithium: 176.0 ± 11.5 %, $p< 0.001$; carbamazepine: 383.2 ± 44.9 %, $p< 0.001$; valproate: 310.3 ± 29.1 %, $p< 0.001$), when compared to the values from control or vehicle-treated rats (Figure 15A).

Forskolin-induced increase in extracellular cAMP was significantly inhibited in the presence of quinpirole, in control and vehicle-treated rats (respectively 187.6 ± 24.6 %, $p< 0.001$ and 282.7 ± 34.4, $p< 0.001$) (Figure 15B a) and d)), as measured 60 min after the infusion of the dopamine D_2-like receptors agonist. However, in lithium- or valproate-treated rats no difference occurred in the forskolin-induced increase in extracellular cAMP in the absence or presence of the agonist (Figure 15B b) and e)) whereas in carbamazepine-treated animals an unexpected increase was observed (885.5 ± 152.7 %, $p< 0.001$) (Figure 15B c)) after infusion of quinpirole plus forskolin, being the obtained value even higher than that observed in control animals under the same conditions (187.6 ± 24.6 %) (Figure 15B a)) or in carbamazepine-treated rats infused only with forskolin (383.2 ± 44.9 %) (Figure 15B c)).

No statistical significant effect on basal cAMP levels neither under control conditions (control rats: 100.4 ± 18.4 %; vehicle-treated rats: 104.0 ± 11.3 %) nor in carbamazepine-treated animals (114.4 ± 8.9 %) was observed after activation of dopamine D_2-like receptors (data not shown).

Taken together, these results indicate that lithium, carbamazepine and valproate, at therapeutically relevant concentrations, modulate basal and forskolin evoked cAMP production. These drugs had no effect on basal cAMP levels in vitro, but differential effects were observed in vivo, in agreement with literature data (Jope,1999a, 1999b; Masana et al., 1991, 1992; Montezinho et al., 2004; Mørk & Jensen, 2000). The different behaviour with cells and in vivo may be due to the lack of afferent projections releasing catecholamines, which could be regulated by the *chronic in vivo* drug infusion (Dziedzicka-Wasylewska et al., 1996; Ichikawa & Meltzer, 1999). Direct stimulation of AC with forskolin increased the levels of cAMP both *in vitro* and *in vivo*, and this effect was significantly inhibited by all three mood stabilizers. Activation of dopamine D_2-like receptors partially inhibited the forskolin-induced increase in cAMP in untreated cell cultures, likely due to AC inhibition (Memo et al., 1992), but no further attenuation in cAMP levels was observed in cultured cortical neurons treated with the three mood-stabilizing drugs, suggesting that, in this case, there are no additive effects, although these drugs can act through different mechanisms (Chen et al., 1996a, 1996b; Gallagher et al., 2004; Montezinho et al., 2004; Mørk & Jensen, 2000; Post et al., 1992).

Similar results were obtained upon chronic *in vivo* treatment with Li⁺ and valproate in the rat prefrontal cortex. However, in carbamazepine-treated animals, the activation of dopamine D_2-like receptors, surprisingly, enhanced the responsiveness of AC to activation by forskolin, possibly due to what is described as super-sensitization of AC, a

neuroadaptative mechanism that occurs under prolonged inhibition of this enzyme (Johnston CA & Watts, 2003). This may have an important role in tolerance and dependency effects generally observed in chronic abuse drugs administration, which are known to induce AC sensitization due to the persistent activation of $G\alpha_i$-coupled receptors. The molecular mechanisms involved in super-sensitization are not completely clarified, however, some studies show that chronic inhibition of PKA induces AC sensitization in some cellular systems and that activation of this kinase has the opposite effect (Johnston et al., 2002).

The down-regulation of the basal cAMP levels by chronic carbamazepine treatment could therefore underlie the sensitization of the dopamine D_2-like receptors in prefrontal cortex *in vivo*. Inhibition of cAMP formation decreases cAMP-dependent PKA activity and inhibits subsequent PKA-mediated phosphorylation events. Recent results demonstrated that chronic inhibition of PKA induced supersensitization of AC in neuronal cell line and that activators of PKA attenuated sensitization. Although inhibition of cAMP and PKA is not generally required for the development of super-sensitization of AC, inhibition of PKA may contribute to the development of sensitization in select cellular models (Johnston et al., 2002).

From these data, it can be speculated that mechanisms such as the sensitization of dopamine D_2-like receptors due to the chronic inhibition of AC by carbamazepine, contribute to the increased relapsed rate observed in patients under monotherapy with this drug for 3-4 years (Post et al., 1990), although it is an effective drug in the acute treatment of bipolar disorder.

In conclusion, abnormal function of brain AC and dopamine systems may be implicated in bipolar disorder. Chronic treatment with lithium, carbamazepine and valproate affects the basal and evoked cAMP levels in a distinct way, both ex vivo and in vivo, resulting in differential responses to dopamine D_2-like receptors activation, and suggesting that additional signalling systems are involved as well.

4.3 The interaction between dopamine D_2-like and β-adrenergic receptors in the prefrontal cortex is altered by mood stabilizing agents

Biogenic monoaminergic neurotransmission has been suggested to be involved in bipolar disorder as well as in the therapy for this disease. The dopamine D_2 receptor is the predominant member of the family of D_2-like dopamine receptors in the brain (Emilien et al., 1999) and the β_1-adrenergic receptors are the most abundant members of β-adrenergic receptors in the cerebral cortex (Rainbow et al., 1984). The effects of the mood stabilizing drugs lithium, carbamazepine or valproate on the intracellular signalling mediated by receptors coupled to activation and inhibition of AC were investigated. Thus, experiments with the dopaminergic and adrenergic systems, particularly on D_2-like and β-adrenergic receptors, respectively positive and negatively coupled to AC, were performed both in cultured rat cortical neurons and in prefrontal cortex of freely moving rats, using microdialysis (Masana et al., 1991, 1992).

Isoproterenol and quinpirole were used to stimulate β-adrenergic and dopamine D_2-like receptors, respectively, and cAMP levels inside neurons and in the dialysates were determined by a radioimmunoassay using the [8-^{3}H-] and [^{125}I], respectively for the *ex vivo*

and *in vivo* experiments. Moreover, the cAMP levels produced by the stimulation of β-adrenergic receptors with isoproterenol as well as the ability of the activation of dopamine D_2-like receptors to block the increase of isoproterenol-evoked cAMP levels were measured under control conditions and after the treatment with mood stabilizing drugs. Immunohistochemistry and western blot techniques were used to investigate if β_1–adrenergic and D_2 dopaminergic receptors are co-localized in the rat prefrontal cortex and if the three drugs have any effect on the levels of these receptors on the membranes of cortical neurons.

The cAMP accumulation in cultured cortical cells is presented (Figure 16), using the experimental conditions described in the legend of the figure.
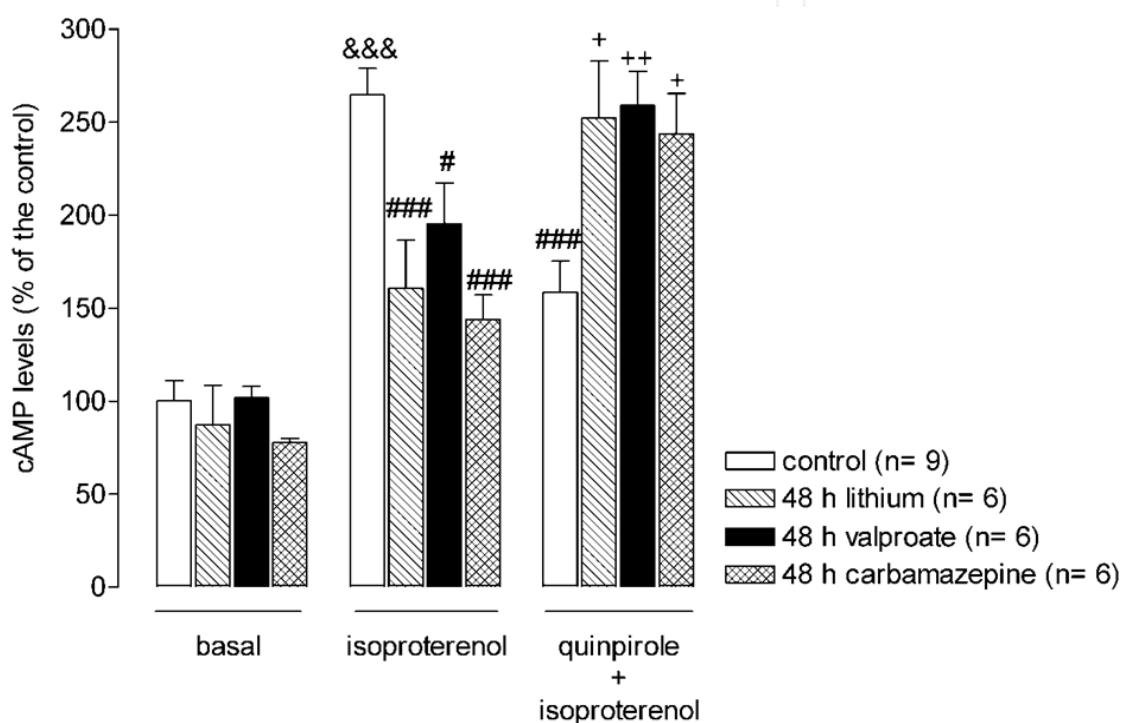
Fig. 16. Effects of lithium, valproate and carbamazepine on the intracellular cAMP levels in cortical neurons under basal conditions and after stimulation with isoproterenol or quinpirole plus isoproterenol. Neurons were pre-exposed or not (control) to 1 mmol L⁻¹ lithium, 0.05 mmol L⁻¹ carbamazepine or 0.5 mmol L⁻¹ valproate, for 48 h. After this period, neurons were incubated with RO-201724 (25 μmol L⁻¹, 15 min) and were then treated or not (basal) with isoproterenol (10 μmol L⁻¹; 15 min), or with isoproterenol together with quinpirole (10 μmol L⁻¹; 15 min). In the latter experimental conditions the cells were pre-treated with 10 μmol L⁻¹ quinpirole for 5 min. The cAMP levels were measured as described (Montezinho et al., 2006). The average value of basal cAMP level for all cells tested (101.4 ± 21.0 nmoL μg⁻¹ protein) was set to 100 %. Data are means ± SEM, for the indicated number of independent experiments, performed in duplicate. Data were analyzed by one-way ANOVA, followed by post-hoc Bonferroni's test for multiple comparisons. ###, p< 0.001; #, p< 0.05 compared to control isoproterenol-treated cells; ⁺, p< 0.05; ⁺⁺, p< 0.01 compared to control quinpirole plus isoproterenol-stimulated cells; &&&, p< 0.001 compared to control of untreated cells; *, p< 0.05; **, p< 0.01 compared to neurons pre-exposed to LiCl and valproate, respectively (Montezinho et al., 2006).

In the *ex vivo* studies, the average value of 101.4 ± 21.0 nmol μg^{-1} protein for basal cAMP level was set to 100 %. Isoproterenol stimulation produced a cAMP increase to 264.6 ± 14.3 %, p< 0.001 (2x above basal levels) which was partially inhibited by lithium, carbamazepine or valproate (lithium: 160.7 ± 25.6 %, p< 0.001; carbamazepine: 143.9 ± 13.1 %, p< 0.001; valproate: 195.4 ± 21.8 %, p< 0.05) although no effect was observed by these drugs on the basal cAMP production. Quinpirole, had no effect on the basal cAMP accumulation (data not shown); however, this dopamine D_2-receptor agonist inhibited isoproterenol-enhanced cAMP levels in untreated neurons (158.4 ± 16.8 %, p< 0.001) and this effect was decreased in neurons pre-exposed to lithium, carbamazepine or valproate (lithium, 249.1 ± 28.4 %, p< 0.05; carbamazepine, 243.8 ± 21.5 %, p< 0.05; valproate, 259.0 ± 18.4 %, p< 0.01) (Figure 16).

To complement these results, in vivo studies were also performed. Preliminary experiments showed that 180 min after probe insertion cAMP levels were stable and were maintained throughout the experiment being the basal cAMP levels for control animals 9.68 ± 2.10 fmol/20 µL, not different in valproate-treated rats, but significantly increased in lithium-treated, 13.17 ± 1.21 fmol/20 µL (p< 0.05) and decreased in carbamazepine-treated rats, 7.82 ± 0.34 fmol/20 µL (p< 0.01).

The concentrations of 2.5 mmol L^{-1} and 100 µmol L^{-1}, respectively, for isoproterenol and quinpirole were used in all in vivo experiments (Figure 17), as they were found to be the minimal concentrations that produced an observable effect under our experimental conditions (Mørk and Geisler, 1994).

After 30 min of isoproterenol infusion in the prefrontal cortex of control and vehicle-treated rats an increase in cAMP levels to, respectively, 234.6 ± 12.2 % and 272.1 ± 12.0 % (Figure 17 A,D) of the basal values occurred, and this effect was significantly decreased in rats pre-treated with the three drugs (lithium: 131.9 ± 5.8 %, p< 0.01; carbamazepine: 159.0 ± 8.5 %, p< 0.01; valproate: 137.9 ± 8.7 %, p< 0.01 (Figure 17 B,C and E). A decrease was also observed in the total isoproterenol-evoked increase in the extracellular cAMP (lithium: 85.1 ± 3.7 %, p< 0.01; carbamazepine: 87. 5 ± 1.6 %, p< 0.05; valproate: 69.5 ± 2.4 %, p< 0.001), when compared to control or vehicle-treated rats values (Figure 17 A,D), similarly to what happened in the *ex vivo* studies. When both isoproterenol and quinpirole were locally infused, the effect of the D_2-like receptors agonist significantly inhibited the effect of isoproterenol-induced increase of extracellular cAMP (control rats: 132.5 ± 5.8 %, p< 0.01; vehicle-treated rats: 141.0 ± 9.1, p< 0.01) measured 30 min after the agonist infusion (control rats: 77.0 ± 1.6 %, p< 0.001; vehicle-treated rats: 74.9 ± 2.7, p< 0.001) (Figure 17 A, D) and the total increase in extracellular cAMP evoked by isoproterenol within 150 min (Figure 17 F)). In lithium-treated rats the activation of D_2-like receptors did not inhibit the isoproterenol-induced increase in extracellular cAMP as demonstrated by measurements 30 min after infusion (188.2 ± 19.1 %, p< 0.01 (Figure 17 B), vs control 132.5 ± 5.8 % (Figure 17 A) or lithium- treated animals infused only with isoproterenol (131.9 ± 5.8 %) (Figure 17 B) and the total extracellular cAMP produced within 150 min (77.0 ± 1.6 vs 94.7 ± 4.4 %, p< 0.01, (Figure 17 F), as it was observed in cortical neuron cultures. In contrast to the behaviour of the three drugs in the *ex vivo* studies and in lithium-treated rats, in carbamazepine- or valproate-treated animals, quinpirole did not significantly change the isoproterenol-induced increase in extracellular cAMP (176.9 ± 8.3 % and 158.0 ± 11.7 %, respectively (Figure 17 C ,E) *vs* control 132.5 ± 5.8 % , vehicle-treated rats 137.9 ± 8.7 %, (Figure 17 A,D), or carbamazepine- 159.0 ± 8.5 % or valproate - treated rats 137.9 ± 8.7 %, and infused only with isoproterenol (Fig. 3C and E) produced 30 min post-infusion, or the total evoked

extracellular accumulation of cAMP measured during 150 min following infusion with quinpirole and isoproterenol (84.7 ± 3.5 % and 85.9 ± 2.2 %, respectively vs control 77.0 ± 1.6 % and vehicle-treated rats 74.9 ± 2.7 %, (Figure 17 F). As a control, it was observed that the activation of D_2-like receptors had no effect on basal cAMP levels under control conditions (control rats: 100.4 ± 18.4 %; vehicle-treated rats: 104.0 ± 11.3 %) but in lithium-treated rats the activation with quinpirole, significantly increased cAMP levels to 155.1 ± 9.3 %, $p < 0.05$ and in carbamazepine- and valproate-treated rats the basal cAMP levels didn't significantly change (114.4 ± 8.9 % and 98.7 ± 13.6 %, respectively vs 100.4 ± 18.4 % and 104.0 ± 11.3 %).
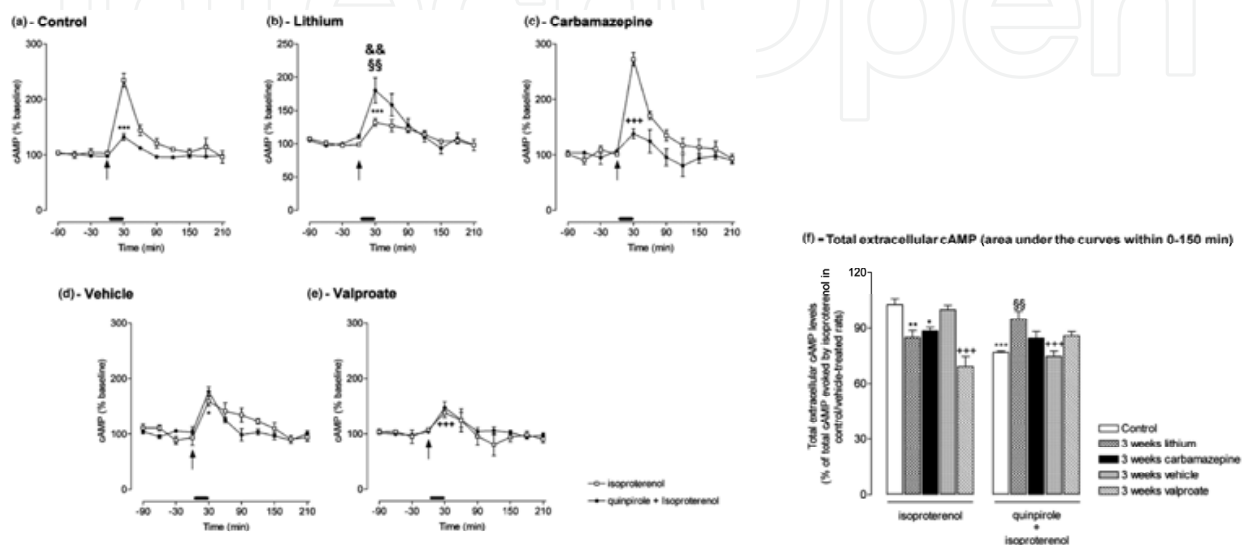
Fig. 17. Effect of the local infusion of isoproterenol (2.5 mmol L^{-1}) or quinpirole (100 µmol L^{-1}) simultaneously with isoproterenol (2.5 mmol L^{-1}) (starting at arrow) on the maximal extracellular cAMP levels produced 30 min post-infusions (a) control rats; b) lithium-treated rats; c) carbamazepine-treated rats; d) vehicle-treated rats; e) valproate-treated rats) and on total cAMP levels (correspondent to the area under the curves), measured within 150 min post-infusions (f). Basal cAMP level was taken as the average cAMP concentration in the four consecutive samples collected from 3 h after the insertion of the probe, prior to isoproterenol (8.9 ± 2.6 fmol/20 µL, n= 6) and quinpirole plus isoproterenol infusions (9.4 ± 1.1 fmol/20 µL, n= 4). Thereafter, the agent of interest (2.5 mmol L^{-1} isoproterenol or 100 µmol L^{-1} quinpirole plus 2.5 mmol L^{-1} isoproterenol) dissolved in Ringer solution was infused through the probe, for 30 min, and seven samples were then collected. Extracellular cAMP levels in the dialysates were measured by radioimmunoassay analysis and expressed as percentages of the basal value (a)-e)) or expressed as a percentage of the percentage of the total amount of cAMP produced during 150 min post-infusion with isoproterenol in control or vehicle-treated rats (f). Results are means ± SEM, from 4 to 6 independent experiments. The rats were treated or not with doses yielding therapeutic plasma levels of lithium, carbamazepine or valproate, during three weeks, as indicated in (Montezinho et al., 2006). Data are analyzed by one-way ANOVA, followed by post-hoc Bonferroni's test for multiple comparisons. ***, $p < 0.001$; compared to the cAMP produced 30 min after the infusion of isoproterenol in control rats. +++, $p < 0.001$; compared to the cAMP produced 30 min after the infusion of isoproterenol in vehicle-treated rats. §§, $p < 0.01$; compared to the cAMP produced 30 min after the infusion of quinpirole plus isoproterenol in control rats. &&, $p < 0.001$; compared to the cAMP produced 30 min after the infusion of quinpirole plus isoproterenol in lithium-treated rats (Montezinho et al., 2006).

Taken together, *ex vivo* and *in vivo* data showed that stimulation of β-adrenergic receptors with isoproterenol increased cAMP levels and this effect was significantly inhibited by lithium, carbamazepine or valproate. The activation of dopamine D_2-like receptors with quinpirole decreased the isoproterenol-induced raise in cAMP in control conditions. This inhibition was observed *in vivo* after chronic treatment of the rats with carbamazepine or valproate, but not after treatment with lithium or in cultured rat cortical neurons after 48 h exposure to the three mood stabilizers.

Immunohistochemistry studies (data not shown) (Montezinho et al., 2006) confirmed the co-existence of dopamine D_2 and $β_1$-adrenergic receptors in the majority of the cells of the rat prefrontal cortex, allowing the interactions at the second messenger level. The results obtained from prefrontal cortex sections of lithium- carbamazepine or valproate-treated suggested a loss of dopamine D_2 receptors, whereas in valproate-, carbamazepine-, and lithium-treated rats the $β_1$-adrenergic receptors seemed to be, respectively, down-regulated, upregulated or not changed (Montezinho et al., 2006).To confirm these data, the levels of the dopamine D_2 and $β_1$-adrenergic receptor proteins were determined in membranes prepared from cultured rat cortical neurons and from rat prefrontal cortex, pre-treated or not with the mood stabilizing agents, by western blot analysis, using the same anti-D_2 and anti-$β_1$ specific antibodies used for immunohistochemistry. An evident immunoreactivity was observed at ≈50 kDa and ≈64 kDa, the predicted molecular weights for the dopamine D_2 and $β_1$ adrenergic receptor proteins, respectively, in protein extracts from cultured rat cortical neurons and from cortex of rats treated with the three drugs (data not shown) (Montezinho et al., 2006). The quantitative analysis of these bands, by densitometry, confirmed that lithium, valproate and carbamazepine treatments significantly decreased dopamine D_2 receptor protein levels in membranes from treated cultured rat cortical neurons and in prefrontal cortex of treated animals when compared with control values. Concerning $β_1$-adrenergic receptors only valproate decreased the expression of the receptor present in cultured cortical neurons; however, *in vivo* treatment with carbamazepine, valproate or lithium, up-regulated, down-regulated or had no effect on $β_1$-adrenergic receptor levels, respectively, when compared with control and vehicle-treated rats (data not shown) (Montezinho et al., 2006).

In conclusion, this study shows that there is a cross-talk between dopamine D_2-like and β-adrenergic receptors activities in the rat brain cortical region, which is differentially affected by therapeutic concentrations of the mood stabilizing drugs lithium, carbamazepine and valproate. Indeed, *in vivo* and *in vitro* data showed that activation of dopamine D_2-like receptors inhibits $β_1$-adrenergic receptor stimulated cAMP production. *Ex vivo* this inhibition was attenuated by lithium, carbamazepine and valproate, whereas *in vivo* only lithium had such effect. Consistent with this regulatory role on AC activity, dopamine D_2 and $β_1$-adrenergic receptors are co-localized in the rat prefrontal cortex and their protein levels are changed by mood stabilizers as determined by immunohistochemistry and immunoblotting, respectively.

These data show that the three mood stabilizers affect dopamine D_2-like receptor-mediated regulation of β-adrenergic signalling, both *ex vivo* and *in vivo* although in a different way. The discrepancy between *ex vivo* and *in vivo* results can be explained through at least three factors: the cellular interactions in the 3D structure of intact rat brain are different from those in a 2D

typical organization of neuronal cultures (Dziedzicka-Wasylewska et al. 1996; Ichikawa & Meltzer 1999); the absence of glial cells, which contain β-adrenergic and D$_2$-like receptors (Stone & John 1990; Stone et al. 1990), in the cortical neuron cultures used; cortical neuron cultures were exposed to the mood stabilizing agents for 48 h whereas the animals were treated with the same drugs during three weeks and, according to literature data, the mechanisms involved in acute and chronic Li$^+$ treatment are different (Mørk & Geisler, 1987b, 1989c; Newman & Belmaker, 1987). This highlights the importance of the *in vivo* studies. Each of these drugs acts by a unique mechanism *in vivo*: chronic treatment with lithium increases cAMP levels which may be attributed to the inhibition of G$_i$, (Jope, 1999a; Masana et al., 1991, 1992; Montezinho et al., 2004); however, taking into account data here presented, the loss of dopamine D$_2$-like receptors, which are coupled to the inhibition of AC, may also account for the increase in the basal cAMP levels, thus mediating lithium antimanic action (Schatzberg et al., 2004; Silverstone and Silverstone, 2004; Yatham *et al.*, 2002),. In contrast with lithium, *in vivo* carbamazepine treatment decreases cAMP levels despite an observed increase in the β$_1$-receptor expression. This effect may be exerted primarily at the level of cAMP production, by the direct inhibition of AC (Chen et al., 1996a), which can also explain the attenuated isoproterenol-evoked cAMP production and the lack of a further effect of D$_2$ receptor activation. The changes in receptor levels could represent a compensatory mechanism in the *in vivo* conditions. *In vivo* administration of valproate significantly reduced both the β$_1$-adrenergic and dopamine D$_2$ receptor levels, which can explain the decrease in isoproterenol-evoked receptor-mediated cAMP production, and no further attenuation of cAMP production after dopamine D$_2$ receptors stimulation. The β-adrenergic down regulation by valproate was also showed *in vitro* (Chen et al., 1996b).

These findings suggest that additional mechanisms are operative *in vivo* as compared to *in vitro*. It can be speculated that dopaminergic and noradrenergic neurotransmitter levels released by afferent projections participate in the regulation of these monoaminergic systems. In agreement with this hypothesis, a decrease in the dopamine concentration in prefrontal cortex and an increase in striatum (Dziedzicka-Wasylewska et al., 1996) were reported after the *in vivo* intragastrical administration of lithium. In contrast, it was described that therapeutic concentrations of carbamazepine or valproate enhanced basal releases of dopamine in the prefrontal cortex (Ichikawa & Meltzer, 1999). In addition, carbamazepine and valproate are metabolized *in vivo*, what might contribute to the differences observed in the effects of these drugs *in vitro* and *in vivo*. Moreover, the presence of glia cells expressing β$_1$-adrenergic (Stone *et al.*, 1990; Stone & John, 1990) and D$_2$ receptors (Khan *et al.*, 2001) in rat brain cortex increases the complexity of the regulation of the cAMP levels *in vivo* when compared with the *in vitro* data. Lastly, the other D$_2$-like receptor subtypes, namely the D$_3$ and D$_4$ receptors, and the β$_2$ and β$_3$-adrenergic receptors may also play a role in the regulation of cAMP levels and the expression pattern of these receptors *in vitro* may be different from the one observed *in vivo*.

It has been described that the function of the β-adrenergic receptor signalling in the striatum and prefrontal cortex depends upon dopaminergic activity (Herve et al., 1990). Thus, treatments affecting dopaminergic neurotransmission can influence the success and the rapidity of action of mood stabilizing drug therapy. These results support the hypothesis that therapeutic intervention in bipolar disorder may be improved by affecting β-adrenergic receptor signalling *via* effects on dopamine D$_2$ receptor pathways.

5. Conclusions

The work presented in this chapter focused on Li^+ effects on several cellular systems and *in vivo*, in particular how it affects intracellular Mg^{2+} binding, cell energy metabolism, GABAergic and glutamatergic neurotransmitter systems, intracellular cAMP levels and their modulating systems, contributing to a better understanding of Li^+ action in bipolar disorder. The results showed that:

- Under depolarising conditions, the Na^+/Ca^{2+} exchanger is proposed to be the new contribution to Li^+ influx, resulting from the activation of L-type voltage-sensitive Ca^{2+} channels, where Li^+ replaces Na^+.
- Li^+ intracellular immobilization is cell type dependent.
- Li^+ is able to displace Mg^{2+} from its intracellular binding sites, providing further evidence for the generality of the ionic Li^+/Mg^{2+} competition mechanism. The extent of Li^+/Mg^{2+} competition was suggested to be cell-type dependent, being affected by differences in Li^+ transport and immobilization properties.
- Li^+ had a remarkable inhibitory effect on the energetic metabolism of glucose in SH-SY5Y cells. The results were consistent with an inhibition of glycolytic and TCA cycle fluxes, with an unchanged intracellular redox state. Li^+ did not interfere with the competitive metabolism of glucose and lactate, or the residual contribution of unlabeled endogenous sources for the acetyl-CoA pool.
  Similarly to SH-SY5Y cells, but to a much lesser extent, neuronal glycolytic flux was also found to be decreased in cultured rat cortical neurons after incubation with 15 mmol L^{-1} Li^+.
- Li^+ decreased the incorporation of ^{13}C labeling into GABA carbons from its precursor glutamate in neurons, both *in vivo* and *ex vivo*, suggesting an inhibitory effect on glutamate decarboxylase.
- Li^+ plays an important role in the homeostasis of the second messenger cAMP in neuronal cells (Fig. 18 B) a.).
- In cultured cortical neurons the mood stabilizing drugs Li^+, valproate and carbamazepine do not affect basal cAMP levels, although *in vivo* different effects are observed. The increase in β-adrenergic- and forskolin-mediated production of cAMP is attenuated by the three drugs both *ex vivo* and *in vivo* (Fig. 18 B) b.).
- The three mood stabilizers act on the dopamine D_2-like and β-adrenergic receptor-mediated regulation of cAMP levels both *in vivo* and *ex vivo* (Fig. 18 B) b.), but by different mechanisms. This may explain the differences in their efficacy in the treatment of manic episodes in clinical cases.

Fig.18 summarizes some of the results obtained concerning targets and effects of Li^+, carbamazepine and valproate.

This work is a contribution to clarify some of the hypotheses that have been advanced for Li^+ action namely the ionic competition model, the effects on energetic metabolism and on signal transduction pathways. Li^+ acts on multiple targets and interferes with many biological processes. Although biological effects cannot be studied isolated, the data presented are some pieces to join the puzzled information in the literature, which hopefully will help to make "the whole story" - a step forward to establish the general mechanism of action of this ion in bipolar disorder.

Multinuclear NMR spectroscopy was found to be a powerful tool in the study of Li$^+$ transport, Li$^+$ immobilization and Li$^+$ effects on different metabolic pathways involved in cell energy production and signalling. Application of mathematical models to ^{13}C NMR data obtained from cultured brain cells and rat brain *in vivo* seems to be a promising strategy to identify, more precisely, the metabolic pathways specifically affected by Li$^+$. Microdialysis in freely moving animals showed to be very useful for the *in vivo* quantification of neurotransmitters, providing information about signal transduction processes.

(A)   (B)
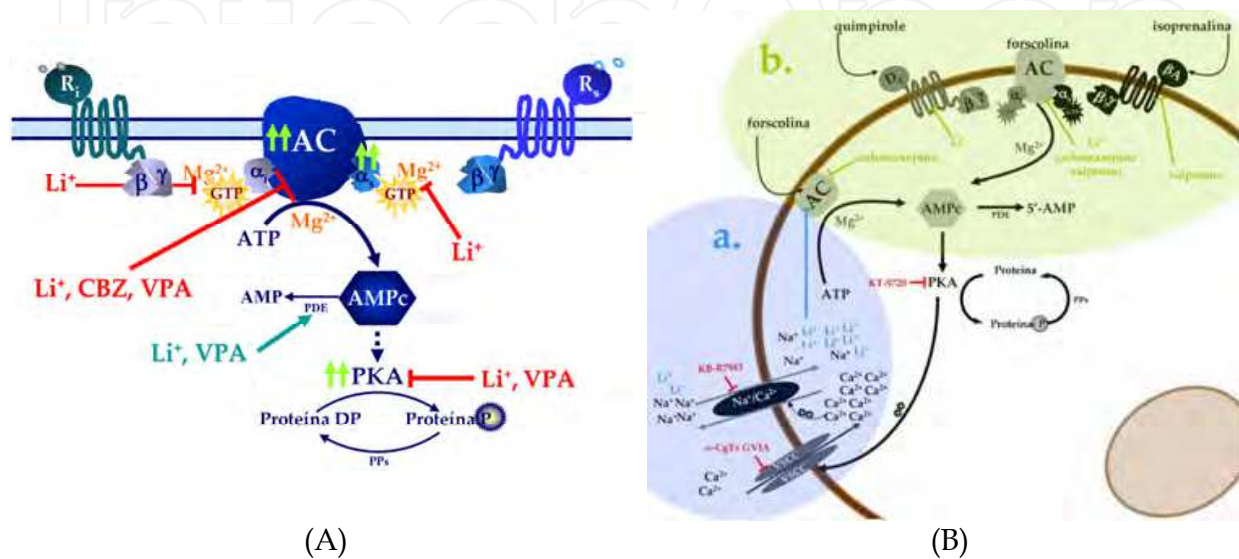
Fig. 18. **A**) Signal transduction cascades involved in the pathophysiology of bipolar disorder (alterations represented by ↑↑) and in the therapeutic action of mood-stabilizing agents (Li$^+$), valproate (VPA) e carbamazepine (CBZ) (represented by the red lines (**inhibition**) and blue arrow (**activation**). Li$^+$ and VPA activate phosphodiesterases (PDE) which hydrolyze 3'5'-cyclic-adenosine monophosphate (cAMP), and the three mood stabilizing agents reduce the activity of adenylate cyclase (AC). Li$^+$ inhibits the activity of stimulatory and inhibitory G proteins (G$_{\alpha s}$ e G$_{\alpha i}$), which is explained through Li$^+$/Mg^{2+}competition. These alterations contribute to the reduction of protein kinase A (PKA) activity decreasing its phosphorylation capacity and originating long term perturbations. Phosphatases (PPs) convert phosphoproteins (P-proteins) in the dephosphorylated form (DP-protein). cAMP is hydrolyzed to 5'-AMP by phosphodiesterases (PDE) (Jope 1999a; Manji *et al.*, 1995, 2001). **B**) **a)** The activation of adenylate cyclase (AC) with forskolin increases Li$^+$ uptake by SH-SY5Y cells and by cultured hippocampal and cortical neurons, at therapeutic concentrations of this cation. The inhibitory of the Na$^+$/Ca^{2+} exchanger, KB-R7943, reduces Li$^+$ influx under resting conditions and completely inhibits the effect of forskolin on the accumulation of this cation. Inhibition of N–type voltage-sensitive Ca^{2+} channels (VSCC), with ω-CgTx GVIA, or inhibition of protein kinase A (PKA) with KT-5720, also abolishes the effect of forskolin on Li$^+$ uptake. The effect of cAMP in SH-SY5Y cells is mediated by PKA and occurs *via* changes in the intracellular free concentration ([Ca^{2+}]$_i$). Accordingly, intracellular accumulation of cAMP seems to increase the [Ca^{2+}]$_i$ due to Ca^{2+} entre through N-VSCC, which activates the Na$^+$/Ca^{2+} (Li$^+$/Ca^{2+} exchanger in order to extrude the Ca^{2+} taken up by the cells. **b)** Direct stimulation of AC with forskolin increase cAMP levels both *in vitro* and *in vivo*, and this effect was significantly inhibited by Li$^+$, valproate and carbamazepine. In carbamazepine-treated animals, the activation of dopamine D$_2$-like receptors enhances the responsiveness of

AC to activation by forskolin, possibly as a consequence of chronic inhibition of the activity of this enzyme. An increase in the activation of AC and cAMP production is described as a super-sensitization of AC. In vivo, each of the mood stabilizing drugs modulates dopamine D_2-like (D_2) and β-adrenergic (βA) receptor-regulated cAMP levels by a distinct mechanism. The effects of carbamazepine are most likely due to direct inhibition of AC, whereas Li^+ may act by affecting dopamine D_2 receptor mediated signalling and valproate by down-regulating β-adrenergic transmission.

6. Acknowledgement

7. References

Abreu, L.A. & Abreu, R.R. (1973). Effect of lithium on brain aconitase activity. *Experientia.* 29, 446-447.

Amari, L., Layden, B., Nikolakopoulos, J., Rong, Q., Mota de Freitas, D., Baltazar, G., Castro, M.M.C.A. & Geraldes C.F.G.C. (1999a). Competition between Li^+ and Mg^{2+} in neuroblastoma SH-SY5Y cells: a fluorescence and ^{31}P NMR study. *Biophys J.*, 76, 2934-2942.

Amari, L., Layden, B., Rong, Q., Geraldes, C.F.G.C. & Mota de Freitas, D. (1999b). Comparison of fluorescence, ^{31}P NMR, and ^7Li NMR spectroscopic methods for investigating Li^+/Mg^{2+} competition for biomolecules. *Anal. Biochem.*, 272, 1-7.

Antonelli, T., Ferioli, V., Lo, G.G., Tomasini, M.C., Fernandez, M., O'Connor, W.T., Glennon, J.C., Tanganelli, S. & Ferraro, L. (2000). Differential effects of acute and short-term lithium administration on dialysate glutamate and GABA levels in the frontal cortex of the conscious rat. *Synapse,* 38, 355-362.

Berns, G. S. & Nemeroff, C. B. (2003). The neurobiology of bipolar disorder. *Am. J. Med. Genet. C. Semin. Med. Genet.*, 123, 76-84.

Biedler, J.L., Helson, L. & Spengler, B.A. (1973). Morphology and growth, tumorigenicity, and cytogenetics of human neuroblastoma cells in continuous culture. *Cancer Res.,* 33, 2643-2652.

Bouzier-Sore, A.K., Serres, S., Canioni, P. & Merle, M. (2003). Lactate involvement in neuron-glia metabolic interaction: ^{13}C-NMR spectroscopy contribution. *Biochimie,* 85, 841-848.

Brambilla, P., Perez, J., Barale, F., Schettini, G. & Soares J.C. (2003). GABAergic dysfunction in mood disorders. *Mol. Psychiatry,* 8, 721-37, 715.

Brunello ,N. & Tascedda, F. (2003). Cellular mechanisms and second messengers: relevance to the psychopharmacology of bipolar disorders. *Int. J. Neuropsychopharmacol.,* 6, 181-189.

Caligiuri, M.P., Brown, G.G., Meloy, M.J., Eberson, S.C., Kindermann, S.S., Frank, L.R., Zorrilla, L.E. & Lohr, J.B. (2003). An fMRI study of affective state and medication on cortical and subcortical brain regions during motor performance in bipolar disorder. *Psychiatry Res.,* 123, 171-182.

Castro, M.M.C.A., Nikolakopoulos, J., Zachariah, C., Freitas, D.M., Stubbs, E.B.Jr., Geraldes, C.F.G.C. & Ramasamy, R. (1996). 7Li NMR Study of Lithium Ion Transport in Perfused Human Neuroblastoma Cells. *Metal Ions in Biology and Medicine*, 4, 192-194.

Chen, G., Pan, B., Hawver, D.B., Wright, C.B., Potter, W,Z. & Manji, H.K, (1996a). Attenuation of cyclic AMP production by carbamazepine. *J.Neurochem.,* 67, 2079-2086.

Chen, G., Manji, H.K., Wrigh,t C.B., Hawver, D.B. & Potter, W.Z .(1996b). Effects of valproic acid on beta-adrenergic receptors, G-proteins, and adenylyl cyclase in rat C6 glioma cells. *Neuropsychopharmacology* , 15, 271-280.

Cooper, D. M., Mons, N. & Karpen, J. W. (1995). Adenylyl cyclases and the interaction between calcium and cAMP signaling. *Nature,* 374, 421-424.

Deicken, R.F., Weiner, M.W. & Fein, G. (1995). Decreased temporal lobe phosphomonoesters in bipolar disorder. *J. Affect. Disord .,*33, 195-199.

Deval, E., Raymond, G. & Cognard, C. (2002.) Na⁺-Ca²⁺ exchange activity in rat skeletal myotubes: effect of lithium ions. *Cell Calcium,* 31, 37-44.

Dringen, R., Peters, H., Wiesinger, H. & Hamprecht, B. (1995). Lactate transport in cultured glial cells. *Dev. Neurosci.,* 17, 63-69.

Dziedzicka-Wasylewska, M., Mackowiak, M., Fijat, K., Wedzony, K. (1996). Adaptive changes in the rat dopaminergic transmission following repeated lithium administration. *J. Neural. Transm.,* 103, 765-776.

Emilien, G., Maloteaux, J. M., Geurts ,M., Hoogenberg, K. *et al.* (1999.) Dopamine receptors-physiological understanding to therapeutic intervention potential. *Pharmacol. Ther.,* 84, 133-156.

Fonseca, C.P., Montezinho, L.P., Baltazar, G., Layden, B., Mota de Freitas, D., Geraldes, C.F.G.C. & Castro, M.M.C.A. (2000). Li⁺ influx and binding, and Li⁺/Mg²⁺ competition in bovine chromaffin cell suspensions as studied by 7Li NMR and fluorescence spectroscopy. *Metal Based Drugs,* 7, 357-364.

Fonseca, C.P., Montezinho, L.P., Nabais, C., Tomé, A.R., Freitas, H., Geraldes, C.F.G.C. & Castro, M.M.C.A. (2004). Effects of Li⁺ transport and intracellular binding on Li⁺/Mg²⁺ competition in bovine chromaffin cells. *Biochim Biophys Acta* (*Mol.Cell Res.*), 1691, 79-90.

Fonseca, C.P., Jones, J.G., Carvalho, R.A., Jeffrey, F.M.H., Montezinho, L.P., Geraldes, C.F.G.C. & Castro, M.M.C.A. (2005). Tricarboxylic acid cycle inhibition by Li+ in the human neuroblastoma SH-SY5Y cell line: a ^{13}C NMR isotopomer analysis. *Neurochemistry Int.*, 47, 385-393.

Fonseca, C.P., Sierra, A, Geraldes, C.F.G.C., Cerdán, S. & Castro, M.M.C.A. (2009). Mechanisms underlying Li+ effects in glutamatergic and GABAergic neurotransmissions in the adult rat brain and in primary cultures of neural cells as revealed by ^{13}C NMR. *J. Neurosci. Res.*, 87, 1046-1055.

Friedman, J.E., Lelkes, P.I., Lavie, E., Rosenheck, K., Schneeweiss, F. & Schneider, A.S. (1985). Membrane potential and catecholamine secretion by bovine adrenal chromaffin cells: use of tetraphenylphosphonium distribution and carbocyanine dye fluorescence. *J. Neurochem.*, 44, 1391-1402.

Gallagher, H.C., Bacon, C.L., Odumeru, O.A., Gallagher, K.F., Fitzpatrick, T., Regan, C.M. (2004). Valproate activates phosphodiesterase-mediated cAMP degradation: relevance to C6 glioma G1 phase progression. *Neurotoxicol Teratol.*, 26, 73-81.

Gil, V.M.S. & Geraldes, C.F.G.C. (1987). Relaxação de spins nucleares, In: *Ressonância Magnética Nuclear*, Fundação Calouste Gulbenkian, Chap. 6, pp. 401-497.

Goodwin, G.M., Cavanagh, J.T., Glabus, M.F., Kehoe, R.F., O'Carroll, R.E. & Ebmeier K.P. (1997). Uptake of 99mTc-exametazime shown by single photon emission computed tomography before and after lithium withdrawal in bipolar patients: associations with mania. *Br. J. Psychiatry*, 170, 426-430.

Gottesfeld, Z. (1976). Effect of lithium and other alkali metals on brain chemistry and behavior. I. Glutamic acid and GABA in brain regions. *Psychopharmacologia*, 45, 239-242.

Gupta, R.K., Benovic, J.L. & Rose, Z.B. (1978). The determination of the free magnesium level in the human red blood cell by ^{31}P NMR. *J. Biol .Chem .*, 253, 6172-6176.

Hassel, B, Sonnewald, U. & Fonnum, F. (1995). Glial-neuronal interactions as studied by cerebral metabolism of [2-13C]acetate and [1-13C]glucose: an ex vivo 13C NMR spectroscopic study. *J. Neurochem.*, 64, 2773–2782.

Herve, D., Trovero, F., Blanc, G., Vezina, P., Glowinski, J., Tassin, J.P. (1990). Involvement of dopamine neurons in the regulation of beta-adrenergic receptor sensitivity in rat prefrontal cortex. *J. Neurochem.*, 54, 1864-1869.

Hough C., Lu S. J., Davis C. L., Chuang D. M. *et al.* (1999). Elevated basal and thapsigargin-stimulated intracellular calcium of platelets and lymphocytes from bipolar affective disorder patients measured by a fluorometric microassay. *Biol. Psychiatry*, 46, 247-255.

Ichikawa, J. & Meltzer, H.Y. (1999). Valproate and carbamazepine increase prefrontal dopamine release by 5-HT$_{1A}$ receptor activation. *Eur. J. Pharmacol.*, 380, R1-R3.

Ikeda A. & Kato T. (2003). Biological predictors of lithium response in bipolar disorder. *Psychiatry Clin. Neurosci.*, 57, 243-250.

Johnston, C. A., Beazely, M. A., Vancura, A. F., Wang, J. K. *et al.* (2002.) Heterologous sensitization of adenylate cyclase is protein kinase A-dependent in Cath.a differentiated (CAD)-D2L cells. *J. Neurochem.*, 82, 1087-1096.

Johnston, CA & Watts, VJ. (2003). Sensitization of adenylate cyclase: a general mechanism of neuroadaptation to persistent activation of Galpha(i/o)-coupled receptors? *Life Sci.*, 73, 2913-2925.

Jope, R.S., Miller, J.M., Ferraro, T.N. & Hare, T.A. (1989). Chronic lithium treatment and status epilepticus induced by lithium and pilocarpine cause selective changes of amino acid concentrations in rat brain regions. *Neurochem. Res.,* 14, 829-834.

Jope, R.S. (1999a). A bimodal model of the mechanism of action of lithium. *Mol Psychiatry,* 4, 21-25.

Jope, R.S. (1999b). Anti-bipolar therapy: mechanism of action of lithium. *Mol. Psychiatry,* 4, 117-128.

Kajda, P.K., Birch, N.J., O'Brien, M.J. & Hullin, R.P. (1979). Rat-brain pyruvate kinase: purification and effects of lithium. *J. Inorg. Biochem.,* 11, 361-366.

Kajda, P.K. & Birch, N.J. (1981). Lithium inhibition of phosphofructokinase. *J. Inorg. Biochem.,* 14, 275-278.

Kao, L.S. & Cheung, N.S. (1990). Mechanism of calcium transport across the plasma membrane of bovine chromaffin cells. *J. Neurochem.,* 54, 1972-1979.

Kaplan, O., Aebersold, P. & Cohen, J.S. (1989). Metabolism of peripheral lymphocytes, interleukin-2-activated lymphocytes and tumor-infiltrating lymphocytes from ^{31}P NMR studies. *FEBS Lett .,* 258, 55-58.

Kato, T., Takahashi, S., Shioiri, T. & Inubushi, T. (1993). Alterations in brain phosphorous metabolism in bipolar disorder detected by in vivo ^{31}P and ^{7}Li magnetic resonance spectroscopy. *J. Affect. Disord .,*27, 53-59.

Kato, T., Inubushi, T. & Kato, N. (1998). Magnetic resonance spectroscopy in affective disorders. *J. Neuropsychiatry Clin. Neurosci.,* 10, 133-147.

Kato, T. & Kato, N. (2000). Mitochondrial dysfunction in bipolar disorder. *Bipolar Disord.,* 2, 180-190.

Kennedy, S.H., Javanmard, M. & Vaccarino, F.J. (1997). A review of functional neuroimaging in mood disorders: positron emission tomography and depression. *Can. J .Psychiatry ,*42, 467-475.

Khan, Z.U., Koulen, P., Rubinstein, M., Grandy, D.K., Goldman-Rakic, P.S. (2001). An astroglia-linked dopamine D$_2$-receptor action in prefrontal cortex. *Proc. Natl. Acad. Sci. U S A.* 98, 1964-1969.

Kitayama, S., Ohtsuki, H., Morita, K., Dohi, T. & Tsujimoto, A. (1990). Bis-oxonol experiment on plasma membrane potentials of bovine adrenal chromaffin cells: depolarizing stimuli and their possible interaction. *Neurosci. Lett.,* 116, 275-279.

Layden, B., Fonseca, C.P., Minadeo, N., Abdullahi, H., Castro, M.M.C.A., Geraldes, C.F.G.C. & Mota de Freitas, D. (1999). Comparison of fluorescence, ^{31}P NMR and ^{7}Li NMR spectroscopic methods for the investigation of Li$^+$/Mg^{2+} competition in a model system and applications to cellular systems, In:: *Lithium - 50 years: recent advances in biology and medicine,* Lukas K.C., Becker R.W. & Gallichio V.S. (Eds.), pp. 45-62, Weidner Publishing, Cheshire, Connecticut, USA.

Layden, B., Diven, C., Minadeo, N., Bryant, F.B. & Mota de Freitas, D. (2000). Li$^+$/Mg^{2+} competition at therapeutic intracellular Li$^+$ levels in human neuroblastoma SH-SY5Y cells. *Bipolar Disorder,* 2, 200-204.

Layden, B.T., Abukhdeir, A.M., Williams, N., Fonseca, C.P., Carroll, L., Castro, M.M.C.A., Geraldes, C.F.G.C., Bryant, F.B. & Mota de Freitas, D. (2003). Effects of Li$^+$ transport and Li$^+$ immobilisation on Li$^+$/Mg^{2+} competition in cells: implications for bipolar disorder. *Biochem. Pharmacol .,* 66, 1915-1924.

Lenox, R.H. & Hahn, C.G. (2000). Overview of the mechanism of action of lithium in the brain: fifty-year update. *J. Clin. Psychiatry,* 61 Suppl 9, 5-15.

Lust, W.D., Schwartz, J.P. & Passonneau, J.V. (1975). Glycolytic metabolism in cultured cells of the nervous system. I. Glucose transport and metabolism in the C-6 glioma cell line. *Mol. Cell. Biochem.*, 8, 169-176.

Malloy, C.R., Sherry, A.D. & Jeffrey, F.M. (1988). Evaluation of carbon flux and substrate selection through alternate pathways involving the citric acid cycle of the heart by ^{13}C NMR spectroscopy. *J. Biol. Chem.*, 263, 6964-6971.

Manji, H.K., Potter, W.Z. & Lenox, R.H. (1995). Signal transduction pathways. Molecular targets for lithium's actions. *Arch. Gen. Psychiatry*, 52, 531-543.

Manji, H.K. & Lenox R. H. (2000a). The nature of bipolar disorder. *J. Clin. Psychiatry* 61 Supp 13, 42-57.

Manji, H.K. & Lenox R. H. (2000b). Signaling: cellular insights into the pathophysiology of bipolar disorder. *Biol. Psychiatry*, 48, 518-530.

Manji, H. K., Moore G. J. & Chen G. (2001). Bipolar disorder: leads from the molecular and cellular mechanisms of action of mood stabilisers. *Br. J. Psychiatry*, 178, S107-S119.

Marcus, S.R., Nadiger, H.A., Chandrakala, M.V., Rao T.I. & Sadasivudu, B. (1986). Acute and short-term effects of lithium on glutamate metabolism in rat brain. *Biochem. Pharmacol.*, 35, 365-369.

Masana, M.I., Bitran, J.A., Hsiao, J.K., Mefford, I.N., Potter, W.Z. (1991). Lithium effects on noradrenergic-linked adenylate cyclase activity in intact rat brain: an *in vivo* microdialysis study. *Brain Res.*, 538, 333-336.

Masana, M.I., Bitran, J.A., Hsiao, J.K., Potter, W.Z. (1992). *In vivo* evidence that lithium inactivates G_i modulation of adenylate cyclase in brain. *J Neurochem.,*, 59, 200-205.

Memo, M., Pizzi, M., Belloni, M., Benarese, M., Spano, P. (1992). Activation of dopamine D_2 receptors linked to voltage-sensitive potassium channels reduces forskolin-induced cyclic AMP formation in rat pituitary cells. *J. Neurochem.*, 59, 1829-1835.

Miles, K., Anthony, D. T., Rubin, L. L., Greengard, P. & Huganir R. L. (1987). Regulation of nicotinic acetylcholine receptor phosphorylation in rat myotubes by forskolin and cAMP. *Proc Natl Acad Sci U S A*, 84, 6591-6595.

Montezinho, L.P., Fonseca, C.P., Geraldes, C.F.G.C., Castro,M.M.C.A. (2002). Quantification and localization of intracellular free Mg^{2+} in bovine chromaffin cells. *Metal Based Drugs*, 9, 69-80.

Montezinho, L.P., Duarte C.B., Fonseca, C.P., Glinka, Y., Layden, B., Mota de Freitas, D., Geraldes, C.F.G.C., Castro, M.M.C.A. (2004). Intracellular lithium and cyclic AMP levels are mutually regulated in neuronal cells. *J Neurochem*, 90, 920-930.

Montezinho, L.P., Castro, M.M.C.A., Duarte C.B., Penschuck,S., Geraldes, C.F.G.C., Mørk, A. (2006). The interaction between dopamine D_2-like and beta-adrenergic receptors in the prefrontal cortex is altered by mood stabilizing agents. *J. Neurochem.*, 96, 1336-1348.

Montezinho, L.P., Mørk, A., Duarte C.B., Penschuck,S., Geraldes, C.F.G.C., Castro, M.M.C.A. (2007). Effect of mood stabilizers on dopamine D2-like receptors-mediated inhibition of adenylate cyclase. *Bipolar Disorders*, 9, 290-297.

Mørk, A. & Geisler, A. (1987). Mode of action of lithium on the catalytic unit of adenylate cyclase from rat brain. *Pharmacol. Toxicol.* 60, 241-248.

Mørk, A. & Geisler, A. (1989). The effects of lithium *in vitro* and *ex vivo* on adenylate cyclase in brain are exerted by distinct mechanisms. *Neuropharmacology*, 28, 307-311.

Mørk, A. & Geisler, A. (1994). Lithium *in situ* decreases extracellular levels of cyclic AMP in the dorsal hippocampus of living rats. *Pharmacol. Toxicol.*, 74, 300-302.

Mørk, A. & Jensen, J. (2000). Effects of lithium and other mood-stabilizing agents on the cyclic adenosine monophosphate signaling system in the brain., In: Bipolar medications. Mechanisms of action. Manji H, Bowden C, Belmaker R (Ed). Washington: American pychiatric press, Inc.,: pp 109-128.

Mota de Freitas, D., Amari, L., Srinivasan, C., Rong, Q., Ramasamy, R., Abraha, A., Geraldes, C.F.G.C. & Boyd, M.K. (1994). Competition between Li⁺ and Mg²⁺ for the phosphate groups in the human erythrocyte membrane and ATP: an NMR and fluorescence study. *Biochemistry*, 33, 4101-4110.

Mota de Freitas, D., Castro, M.M.C.A. & Geraldes, C.F.G.C. (2006). Is Competition Between Li⁺ and Mg²⁺ the Underlying Theme in the Proposed Mechanisms for the Pharmacological Action of Lithium Salts in Bipolar Disorder? *Acc. Chem. Res.*, 39, 283-291.

Newman M. E. & Belmaker R. H. (1987) Effects of lithium *in vitro* and *ex vivo* on components of the adenylate cyclase system in membranes from the cerebral cortex of the rat. *Neuropharmacology* 26, 211-217.

Nikolakopoulos, J., Zachariah, C., Mota de Freitas, D. & Geraldes, C.F.G.C. (1996). Comparison of the use of gel threads and microcarrier beads in Li⁺ transport studies of human neuroblastoma SH-SY5Y cells. *Inorg. Chim. Acta,* 251, 201-205.

Nikolakopoulos, J., Zachariah, C., Mota de Freitas, D., Stubbs, E.B., Ramasamy, R., Castro, M.M.C.A. & Geraldes, C.F.G.C. (1998). ⁷Li nuclear magnetic resonance study for the determination of Li⁺ properties in neuroblastoma SH-SY5Y cells. *J .Neurochem.*, 71, 1676-1684.

Njus, D., Sehr, P.A., Radda, G.K., Ritchie, G.A. & Seeley P.J. (1978). Phosphorus-31 nuclear magnetic resonance studies of active proton translocation in chromaffin granules. *Biochemistry*, 17, 4337-4343.

Nordenberg, J., Kaplansky, M., Beery, E., Klein, S. & Beitner, R. (1982). Effects of lithium on the activities of phosphofructokinase and phosphoglucomutase and on glucose-1,6-diphosphate levels in rat muscles, brain and liver. *Biochem. Pharmacol.*, 31, 1025-1031.

O'Donnell, T., Rotzinger, S., Ulrich, M., Hanstock, C.C., Nakashima, T.T. & Silverstone, P.H. (2003). Effects of chronic lithium and sodium valproate on concentrations of brain amino acids. *Eur Neuropsychopharmacol,* 13, 220-227.

Otero Losada, M.E. & Rubio, M.C. (1986). Acute and chronic effects of lithium chloride on GABA-ergic function in the rat corpus striatum and frontal cerebral cortex. *Naunyn Schmiedebergs Arch. Pharmacol.*, 332, 169-172.

Painter, G.R., Diliberto, E.J., Jr. & Knoth, J. (1989). ³¹P nuclear magnetic resonance study of the metabolic pools of adenosine triphosphate in cultured bovine adrenal medullary chromaffin cells. *Proc. Natl .Acad. Sci .U S A*, 86, 2239-2242.

Pellerin, L. & Magistretti, P.J. (2004). Neuroscience. Let there be (NADH) light. *Science,* 305, 50-52.

Petty, F. (1995). GABA and mood disorders: a brief review and hypothesis. *J. Affect. Disord.*, 34, 275-281.

Plenge, P. (1976). Acute lithium effects on rat brain glucose metabolism - *in vivo. Int. Pharmacopsychiatry,* 11, 84-92.

Post, R.M., Leverich, G.S., Rosuf,f A.S. (1990). Carbamazepine prophylaxis in refractory affective disorders: a focus on long-term follow-up. *J. Clin. Psychopharmacol.*, 10, 318–327.

Post, R.M., Weiss, S.R., Chuang, D.M. (1992). Mechanisms of action of anticonvulsants in affective disorders: comparisons with lithium. *J. Clin. Psychopharmacol.*, 12, 23S-35S.

Powis, D.A., O'Brien, K.J. & Von Grafenstein, H.R. (1991). Calcium export by sodium-calcium exchange in bovine chromaffin cells. *Cell Calcium,* 12, 493-504.

Rainbow, T.C., Parsons, B. & Wolfe, B.B. (1984). Quantitative autoradiography of beta 1- and beta 2-adrenergic receptors in rat brain. *Proc.Natl.Acad.Sci.U.S.A,* 81, 1585-1589.

Raju B., Murphy E., Levy L.A., Hall R.D. and London R.E. (1989) A fluorescent indicator for measuring cytosolic free magnesium. *Am J Physiol* 256, C540-C548.

Ramasamy, R. & Mota de Freitas, D. (1989). Competition between Li^+ and Mg^{2+} for ATP in human erythrocytes. A ^{31}P NMR and optical spectroscopy study. *FEBS Lett.,* 244, 223-226.

Rodrigues, T.B. & Cerdán, S. (2005). ^{13}C MRS: an outstanding tool for metabolic studies. *Concepts Magnet Reson*, 27A, 1–16.

Rong, Q., Espanol, M., Mota de Freitas, D. & Geraldes, C.F.G.C. (1993). ^7Li NMR relaxation study of Li^+ binding in human erythrocytes. *Biochemistry,* 32, 13490-13498.

Rong, Q., Mota de Freitas, D. & Geraldes, C.F.G.C. (1994). Competition between lithium and magnesium ions for the substrates of second messenger systems: a nuclear magnetic resonance study. *Lithium,* 5, 147-156.

Rubio, M.C. & Otero Losada, M.E. (1986). GABAergic responses to lithium chloride: dependence on dose, treatment length and experimental condition. *Adv. Biochem. Psychopharmacol.,* 42, 69-77.

Schatzberg, A.F. (2004). Employing pharmacologic treatment of bipolar disorder to greatest effect. *J.Clin.Psychiatry* 65, 15-20.

Sherry, A.D., Jeffrey, F.M. & Malloy C.R. (2004). Analytical solutions for ^{13}C isotopomer analysis of complex metabolic conditions: substrate oxidation, multiple pyruvate cycles, and gluconeogenesis. *Metab. Eng.,* 6, 12-24.

Shiah, I.S. & Yatham, L.N. (1998). GABA function in mood disorders: an update and critical review. *Life Sc.i* 63, 1289-1303.

Silverstone, P.H. & Silverstone, T. (2004). A review of acute treatments for bipolar depression. *Int.Clin.Psychopharmacol.,* 19, 113-124.

Silverstone, P. H., McGrath, B. M., Wessels, P. H., Bell, E. C. *et al.* (2005). Current pathophysiological findings in bipolar disorder and in its subtypes. *Curr. Psychiatric Reviews,* 1, 75-101.

Sonnewald, U. & Kondziella, D. (2003). Neuronal glial interaction in different neurological diseases studied by *ex vivo* ^{13}C NMR spectroscopy. *NMR Biomed.,* 16, 424-429.

Srinivasan, C., Minadeo, N., Geraldes, C.F.G.C. & Mota de Freitas, D. (1999). Competition between Li^+ and Mg^{2+} for red blood cell membrane phospholipids: A ^{31}P, ^7Li, and ^6Li nuclear magnetic resonance study. *Lipids,* 34, 1211-1221.

Stone, E. A. & John, S. M. (1990). *In vivo* measurement of extracellular cyclic AMP in the brain: use in studies of beta-adrenoceptor function in nonanesthetized rats. *J. Neurochem.* 55, 1942-1949.

Stone, E. A., Sessler, F. M. & Liu, W. M. (1990). Glial localization of adenylate-cyclase-coupled beta-adrenoceptors in rat forebrain slices. *Brain Res.,* 530, 295-300.

Trifaró, J.M. (1982). The cultured chromaffin cell: a model for the study of biology and pharmacology of paraneurones. *Trends Pharmacol. Sci.,* 3, 389-392.

Waniewski, R.A. & Martin, D.L. (1998). Preferential utilization of acetate by astrocytes is attributable to transport. *J. Neurosci.,* 18, 5225-5233.

Yatham, L.N. (2002). The role of novel antipsychotics in bipolar disorders. *J.Clin.Psychiatry,* 63, 10-14.

Zager, E.L. & Ames, A., III (1988). Reduction of cellular energy requirements. Screening for agents that may protect against CNS ischemia. *J. Neurosurg.,* 69, 568-579.
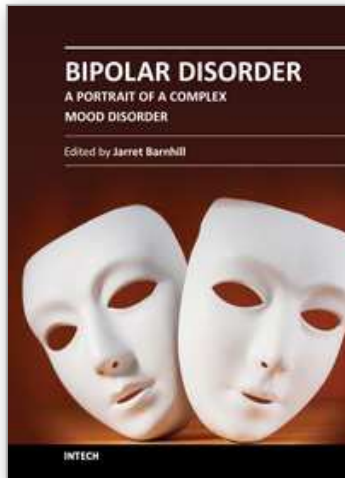
Bipolar Disorder - A Portrait of a Complex Mood Disorder

Edited by Dr. Jarrett Barnhill

Bipolar Disorder: Portrait of a Complex Mood Disorder is a step towards integrating many diverse perspectives on BD. As we shall see, such diversity makes it difficult to clearly define the boundaries of BD. It is helpful to view BD from this perspective, as a final common pathway arises from multiple frames of reference. The integration of epigenetics, molecular pharmacology, and neurophysiology is essential. One solution involves using this diverse data to search for endophenotypes to aid researchers, even though most clinicians prefer broader groupings of symptoms and clinical variables. Our challenge is to consolidate this new information with existing clinical practice in a usable fashion. This need for convergent thinkers who can integrate the findings in this book remains a critical need. This book is a small step in that direction and hopefully guides researchers and clinicians towards a new synthesis of basic neurosciences and clinical psychiatry

How to reference

In order to correctly reference this scholarly work, feel free to copy and paste the following:

Carla P. Fonseca, Liliana P. Montezinho and"M. Margarida C.A. Castro (2012). Li+ in Bipolar Disorder – Possible Mechanisms of Its Pharmacological Mode of Action, Bipolar Disorder - A Portrait of a Complex Mood Disorder, Dr. Jarrett Barnhill (Ed.), ISBN: 978-953-51-0002-7, InTech, Available from: http://www.intechopen.com/books/bipolar-disorder-a-portrait-of-a-complex-mood-disorder/li-in-bipolar-disorder-possible-mechanisms-of-its-pharmacological-mode-of-action

INTECH
open science | open minds